Dissertation
submitted to the
Combined Faculties for the Natural Sciences and for Mathematics
of the Ruperto-Carola University of Heidelberg, Germany
for the degree of
Doctor of Natural Sciences

Presented by

Hanna Korhonen (MSc)
Born in: Joensuu, Finland
Oral examination: ……..

ANALYSIS OF G_q/G_{11} AND G_{12}/G_{13} MEDIATED SIGNALLING IN THE ENDOTHELIAL FUNCTIONS

Referees: Prof. Dr. Stefan Offermanns

Prof. Dr. Markus Schwaninger

TABLE OF CONTENTS

1 ABBREVIATIONS

BSA	bovine serum albumin
GPCR	G-protein coupled receptor
EtOH	ethanol
KO	knock-out
MLC	myosin light chain
MLCP	myosin light chain phosphatase
MLCK	myosin light chain kinase
NO	nitric oxide
PAF	platelet activating factor
PBS	phosphate buffer
PKC	protein kinase C
PLC	phospholipase C
ROCK	Rho kinase
WT	wild-type

2 SUMMARY

In this study, I analyzed the role of GPCR signalling pathways mediated by G_q/G_{11} and G_{12}/G_{13} in the functions of the adult endothelium. To achieve endothelium specific deletion of $G\alpha_{q/11}$ and $G\alpha_{12/13}$, I crossed an inducible Tie2-Cre mouse line with mice carrying floxed alleles of the genes encoding $G\alpha_q$ (*Gnaq*) and $G\alpha_{13}$ (*Gna13*) in $G\alpha_{11}$- or $G\alpha_{12}$-deficient backgrounds, respectively. After induction of Cre with tamoxifen, I observed endothelium specific recombination in various organs, excluding brain vessels and aorta. I confirmed the loss of $G\alpha_{q/11}$ and $G\alpha_{12/13}$ in pulmonary endothelial cells isolated from the respective mouse lines and was able to show that the phosphorylation of MLC in primary pulmonary endothelial cells depended on $G\alpha_{q/11}$, while $G\alpha_{12/13}$ pathway was less important. When stimulated with histamine or PAF, endothelial NO production was blocked in the absence of $G\alpha_{q/11.}$ *In vivo* the lack of $G\alpha_{q/11}$ in endothelial cells led to reduced vascular permeability, which was consistent with *in vitro* MLC phosphorylation results. $G\alpha_{q/11}$ was necessary for normal hypotensive response to histamine stimulation, and for PAF-induced shock. Sensitized endothelial cell specific $G\alpha_{q/11}$ KO mice were resistant to development of anaphylactic shock when challenged with allergen. In addition, endothelial $G\alpha_{q/11}$ KO mice showed reduced leukocyte rolling in trauma induced acute inflammation. In conclusion, I was able to show that endothelial $G\alpha_{q/11}$ is a regulator of endothelial cell contraction and endothelial barrier function in response to various inflammatory mediators, and that it is critically involved in systemic anaphylactic reactions. These data suggest that G_q/G_{11}-mediated signalling pathway in endothelial cells is a promising target to prevent or to treat anaphylactic shock.

3 ZUSAMMENFASSUNG

In diesem Forschungsprojekt habe ich die Rolle von G_q/G_{11}- und G_{12}/G_{13}-vermittelten GPCR Signalwegen im Rahmen der Funktion des adulten Endothels analysiert. Um eine Endothel-spezifische Deletion der für $G\alpha_{q/11}$ und $G\alpha_{12/13}$ kodierenden Gene zu erhalten, kreuzte ich eine induzierbare Tie2-Cre Mauslinie mit Mäusen mit gefloxten Allelen der $G\alpha_q$ (*Gnaq*) und $G\alpha_{13}$ (*Gna13*) kodierenden Gene sowohl mit $G\alpha_{11}$- oder $G\alpha_{12}$-defizientem Hintergrund. Nach Induktion von Cre mittels Tamoxifen konnte ich eine Endothel-spezifische Rekombination in verschiedenen Organen, nicht aber in Hirngefäßen und Aorta, beobachten. Ich bestätigte den Verlust von $G\alpha_{q/11}$ und $G\alpha_{12/13}$ in pulmonalen Endothelzellen, die aus den entsprechenden Mauslinien isoliert wurden, und konnte zeigen, dass die Phosphorylierung von MLC in primären pulmonalen Endothelzellen abhängig war von $G\alpha_{q/11}$, während der $G\alpha_{12/13}$ Signalweg eine deutlich geringere Rolle spielte. Die Stimulation der endothelialen NO-Produktion durch Histamin oder PAF war in Abwesenheit von $G\alpha_{q/11}$ blockiert. *In vivo* führte das Fehlen von $G\alpha_{q/11}$ in Endothelzellen zu einer reduzierten vaskulären Permeabilität, was mit den *in vitro* Ergebnissen der Phosphorylierung übereinstimmte. Endotheliales $G\alpha_{q/11}$ war für eine normale hypotensive Antwort auf eine Histaminstimulierung und für den PAF-induzierten Schock erforderlich. Sensibilisierte Endothelzell-spezifische $G\alpha_{q/11}$ KO-Mäuse waren bei Allergeneinwirkung gegen die Entwicklung eines anaphylaktischem Schock resistent. Zusätzlich zeigten endotheliale $G\alpha_{q/11}$ KO-Mäuse ein reduziertes Leukozyten-“rolling” bei Trauma-induzierter akuter Entzündung. Als diesen Befunden kann geschöußfolgert werden, dass endotheliales $G\alpha_{q/11}$ ein Regulator der endothelialen Zellkontraktion und endothelialen Barrierefunktion als Antwort auf verschiedene entzündliche Mediatoren ist, und dass es eine bedeutende Rolle bei systemischen anaphylaktischen Reaktionen spielt. Diese Daten legen nahe, dass der G_q/G_{11}-vermittelte Signalweg in Endothelzellen eine vielversprechende Zielstruktur für die Prävention oder Behandlung des anaphylaktischen Schocks darstellt.

4 INTRODUCTION

The endothelial cells line all the vessels in every organ and cover a surface area up to 7 m^2 [1]. The existence of a vessel network became clear shortly after the discovery of circulating blood [2]. The first view of the endothelium described it as a passive barrier physically separating the blood and tissue. Since then more information on the functions of endothelium have become available, and the view of the role of endothelium has broadened. Currently the endothelium is considered to be a heterogeneous, disseminated organ that dynamically participates to vital secretory, synthetic, metabolic, and immunologic functions [2].

The integrity of the endothelial barrier is regulated by chemical stimuli or by mechanical stress caused by blood flow [3]. Many mediators that are able to affect the permeability of the endothelial barrier act through the receptors coupled to members of the G-protein families $G\alpha_q$ and $G\alpha_{12}$. Some members of these G-protein families regulate the contractility of the endothelial cells, stress fiber formation, as well as disruption of the cell junctions via the second messenger Ca^{2+}, or small GTPases, such as RhoA and Rac1.

Endothelium controls vascular tone by releasing mediators that influence vascular hemodynamics under physiological conditions. Endothelium secretes vasodilators including nitric oxide (NO), prostacyclin (PGI_2), and platelet activating factor (PAF), as well as vasoconstrictors, such as endothelin-1, which contribute to the regulation of blood pressure and blood flow. These mediators are either synthesized in response to external stimuli (PGI_2, PAF, and endothelin-1), or are constitutively secreted (NO), but the production of the mediator is modulated by external stimuli. Upregulated NO release is associated with a severe allergic

reaction, anaphylactic shock, and it is one of the mediators contributing to vasodilatation during it.

In addition to the above mentioned functions, the endothelium participates to the recruitment of leukocytes into inflamed tissue. Endothelial cells express cell surface-molecules that capture immune cells from the circulation and direct them to the sites of inflammation. These cell-surface molecules are upregulated in response to inflammatory stimuli, and initiate and support the rolling, adhesion, and transmigration of leukocytes.

4.1 The G-protein mediated activation of endothelial cells

4.1.1 The G-protein-mediated signalling system

Heterotrimeric guanine nucleotide-binding proteins (G-proteins) are signal transducers that couple a variety of receptors to effectors, for instance enzymes and ion channels [4, 5]. G-proteins consist of an α-subunit that binds and hydrolyzes guanosine triphosphate (GTP), and of a tightly associated complex formed by β- and γ-subunits that works as a functional unit [6, 7]. The α-subunit defines the identity of G-protein. More than twenty α-subunits have been described, and they can be divided into four families ($G\alpha_s$, $G\alpha_{i/o}$, $G\alpha_q$, and $G\alpha_{12}$) based on sequence homology [8]. The expression pattern of G-protein α-subunits is variable. Some α-subunits are expressed in a very restricted manner. Other α-subunits are expressed in a wide variety of tissues or ubiquitously [10]. Here only the $G\alpha_q$ and $G\alpha_{12}$ families are described.

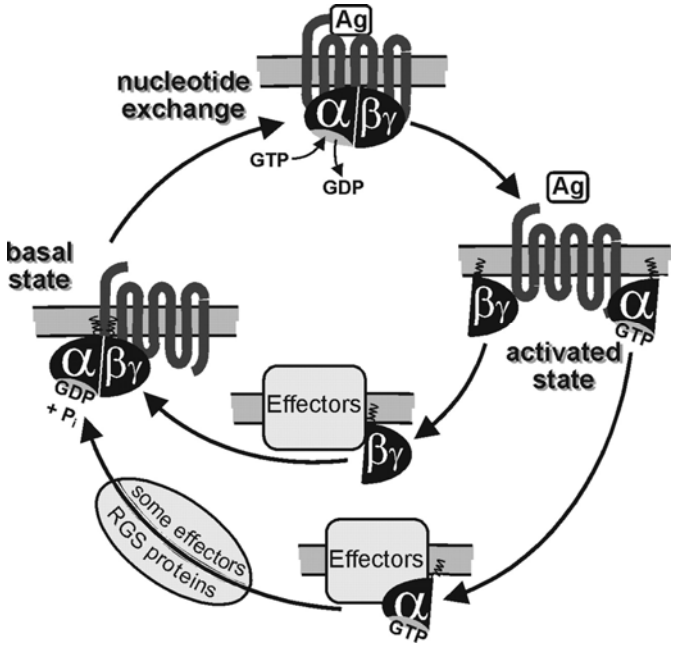

Figure 1. Activation and inactivation cycle of heterotrimeric G-proteins [9]. Described in the text.

In order to transduce a signal from an activated receptor to an effector, the heterotrimeric G-protein undergoes an activation-inactivation-cycle (Figure 1). In the basal state, the guanosine diphosphate (GDP)-bound α-subunit and the complex formed by β- and γ–subunits are associated. In this associated form an activated receptor can recognise the G-protein. The interaction of the receptor and the G-protein heterotrimer leads to the dissociation of GDP from the α-subunit, and to replacement of GDP by GTP. Binding of GTP induces a conformational change in the α-subunit, which results in the dissociation of α-subunit and $\beta\gamma$-complex. Both α-subunit and $\beta\gamma$-complex can now interact with effectors and regulate their functions. This process is terminated by GTPase activity that leads to formation of GDP. GDP binds the α-subunit and allows it to associate with $\beta\gamma$-complex again, which in turn inactivates the $\beta\gamma$-complex.

4.1.2 The $G\alpha_q$-family of G-proteins

The $G\alpha_q$ family consists of four members: $G\alpha_q$, $G\alpha_{11}$, $G\alpha_{14}$, and $G\alpha_{15/16}$. The G-protein α-subunits $G\alpha_q$ and $G\alpha_{11}$ are ubiquitously expressed [11, 12], while $G\alpha_{14}$ and $G\alpha_{15/16}$ are expressed in a rather restricted manner. $G\alpha_{14}$ is expressed in kidney, lung, and spleen, and the expression of human $G\alpha_{16}$ and its murine ortholog $G\alpha_{15}$ is restricted to the hematopoietic system [9]. The members of the $G\alpha_q$ family are known to activate the β-subunit of the phospholipase C (PLC-β) and to be pertussis toxin insensitive [11, 12]. Receptors activating $G\alpha_q$ and $G\alpha_{11}$ do not discriminate between them [13, 14], and there is also no difference in the ability of these G-protein α-subunits to activate PLC β-isoforms [9]. $G\alpha_q$ and $G\alpha_{11}$ both activate the β_1-, β_3-, and β_4-isoforms of PLC, but are poor activators of the PLC β_2-isoform [12]. However, *Pasteurella Multocida* toxin stimulated activation of PLC was shown to be mediated by $G\alpha_q$ alone, and not by $G\alpha_{11}$ [15]. Stimulation of PLC-β leads to increase in intracellular Ca^{2+} concentration and activation of protein kinase C (PKC).

The functions of $G\alpha_q$ and $G\alpha_{11}$ in various biological processes are well established, while the importance of $G\alpha_{14}$ and $G\alpha_{15/16}$ is still unclear. $G\alpha_q$ and $G\alpha_{11}$ were shown to be involved in development of nervous and cardiac systems, as addressed by the studies in mice lacking these G-protein α-subunits. $G\alpha_q$ deficient mice suffered from ataxia and showed typical signs of motor discoordination [16], while double deficient $G\alpha_q/G\alpha_{11}$ mice died at approximately embryonic day 10.5 due to cardiomyocyte hypoplasia [17]. In contrast, $G\alpha_{11}$ deficient mice showed no apparent behavioural or morphological defects, and were viable and fertile. Deletion of $G\alpha_q/G\alpha_{11}$ specifically in cardiomyocytes prevented the development of cardiac hypertrophy caused by pressure overload [18]. The lack of $G\alpha_{15}$ had no

obvious effects; the $G\alpha_{15}$–deficient mice had no defects in haematopoiesis and showed normal inflammatory response [19].

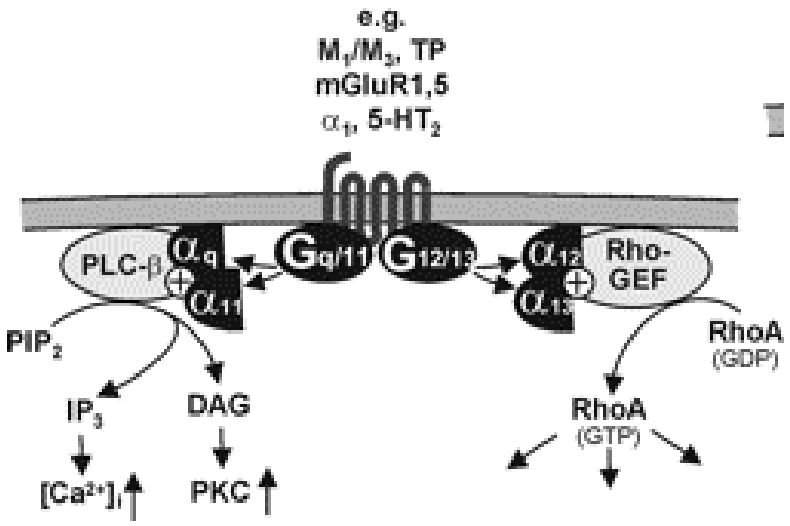

Figure 2. Downstream signalling of $G\alpha_{q/11}$ and $G\alpha_{12/13}$ [9]. Binding of an agonist to a $G\alpha_{q/11}$- or $G\alpha_{12/13}$-coupled receptor leads to activation of PLC-β and increase in intracellular Ca^{2+} concentration and PKC activation, or activation of RhoA, respectively. *M_1/M_3*: muscarinic acetylcholine receptor subtypes 1 and 3, *TP*: thromboxane A_2 receptor, *mGluR1, 5*: metabotropic glutamate receptor subtypes 1 and 5, *α1*: α1-adrenergic receptor, *5-HT_2*: serotonin receptor subtype 2, *PLC-β*: phospholipase C-β,*PIP_2*: phosphatidylinositol 4,5 biphosphate, *IP_3*: inositol 1,4,5-triphosphate, *DAG*: diacylglycerol, *PKC*: protein kinase C, *RhoGEF*: Rho-guanine nucleotide exchange factor.

4.1.3 The $G\alpha_{12}$-family of G-proteins

$G\alpha_{13}$ and $G\alpha_{12}$, the members of the $G\alpha_{12}$ family, are ubiquitously expressed and share 67 % amino acid identity [20]. Due to the lack of specific inhibitors for $G\alpha_{13}$ and $G\alpha_{12}$, the analysis of cellular signalling processes mediated by these G-proteins has faced difficulties. $G\alpha_{12/13}$ are also often activated by receptors coupling to $G\alpha_{q/11,}$ and in addition usually activate other G proteins [9]. Most knowledge on $G\alpha_{12/13}$ regulated cellular functions was therefore gained from over-expression studies, which identified $G\alpha_{12/13}$ as an activator of various downstream effectors such as phospholipase A_2, Na^+/H^+ exchanger, and *c-jun* NH_2-terminal kinase [21-23]. Another important function of $G\alpha_{12/13}$ are their ability to activate the small GTPase

RhoA, which regulates the remodelling of the actin cytoskeleton and stress fiber formation [24]. A subgroup of guanine nucleotide exchange factors (GEFs), consisting of p115-RhoGEF, PDZ-RhoGEF, and LARG, mediates the activation of RhoA [25-27]. PDZ-RhoGEF and LARG are activated by $G\alpha_{13}$ and $G\alpha_{12}$, but p115-RhoGEF is activated by $G\alpha_{13}$ alone. Interestingly, $G\alpha_{12/13}$ are linked with cadherin-mediated signalling, and by interaction with the cytoplasmic domain of some cadherins promote dissociation of β-catenin and cadherin [28, 29].

More information on $G\alpha_{12/13}$-mediated signalling has been collected from studies in genetically modified mice. $G\alpha_{13}$ was found to be important for vascular development. The classical $G\alpha_{13}$ knock-out mice suffered from unorganized vascular system and bleeding resulting in death of the embryos at embryonic day 9.5 [30]. Similarly, endothelial cell specific $G\alpha_{13}$ knock-out mice died between embryonic days 9.5-11.5, and their phenotype was comparable to the phenotype of classical $G\alpha_{13}$ knock-out mice, although less severe [31]. This further suggested an important role for $G\alpha_{13}$ in endothelial cells during embryonic development. In addition, both phenotypes resembled the phenotype of PAR1 knock-out mice [32, 33], which suggested a potential role for $G\alpha_{13}$ as a candidate mediating PAR1 signalling in vascular development. In contrast the classical $G\alpha_{12}$ knock-out mice showed no obvious phenotype, which indicated that $G\alpha_{13}$ was able to compensate for the loss of $G\alpha_{12.}$ The $G\alpha_{12}$/$G\alpha_{13}$ double deficient mice died already *in utero* at E8.5 [34].

4.2 Regulation of endothelial barrier permeability

4.2.1 Structure of interendothelial junctions

Different junctional proteins connect endothelial cells to each other at interendothelial junctions. These include adherens junctions (AJs) and tight junctions (TJs) that are found at the cell borders, where they form a zipperlike structure, and are responsible for adhesion of the adjacent cells to each other. AJs and TJs are the most common types of junctions in both endothelial and epithelial cells [35]. Gap junctions (GJs) form transmembrane channels between cells and can thereby mediate intercellular signalling [35]. The organisation of endothelial junctions varies depending on the permeability requirements of specific tissue or organ [35]. TJs are unorganised in the postcapillary venules, which are sensitive to permeability inducing agonists, and where the trafficking of cells and plasma proteins takes place [35]. In contrast TJs are well organised in the brain, where the permeability of endothelial monolayer is strictly controlled [36].

4.2.1.1 **Adherens junctions**

Endothelial barrier predominantly consists of AJs that are composed of endothelial cell specific vascular endothelial (VE) cadherin and catenin [37], and regulate endothelial barrier function [38]. VE-cadherin is not expressed in any other cell type including blood cells and haematopoietic stem cells [39]. The expression of VE-cadherin starts during development, when endothelial cells become committed to the endothelial lineage [40]. VE-cadherin has 5 cadherin-like repeats that associate with VE-cadherin on the neighbouring cell in a homotypic manner [38]. The association of VE-cadherins is Ca^{2+}-dependent [38]. At interendothelial AJs VE-cadherin forms a cadherin-catenin complex with α- and β-catenins and p120-catenin, which links it to the actin cytoskeleton [39]. The C-terminal domain of VE-cadherin binds α- and β-catenins, and the juxtamembrane domain binds p120-

catenin [39]. Normal endothelial barrier function and AJ assembly require VE-cadherin. Deletion of VE-cadherin in mice led to embryonic lethality and the mice died at E9.5 due to immature vascular development [41, 42]. Vascular permeability increased when functions of VE-cadherin were inhibited *in vivo* by VE-cadherin antibody [38]. Catenins also regulate the assembly of AJs. Truncation of β-catenin binding cytosolic domain of VE-cadherin was lethal in mice [41], and conditional inactivation of β-catenin in endothelial cells led to disability of endothelial cells to maintain cell-to-cell contacts [43].

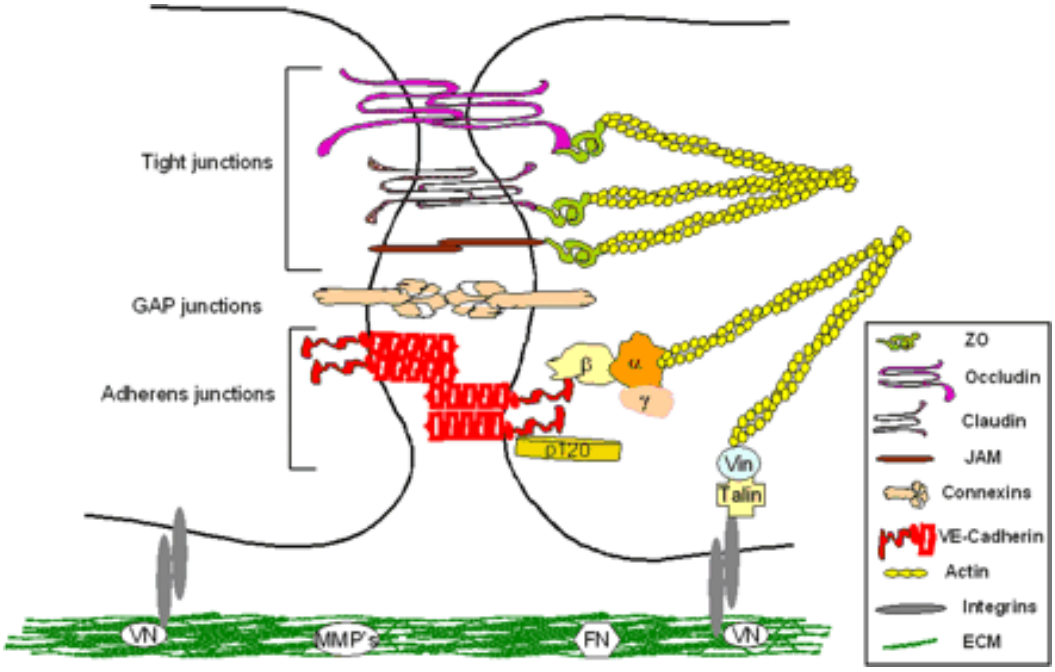

Figure 3. Structure of interendothelial junctions [38]. Shown are the junctional proteins that compose tight junctions, GAP junctions, and adherens junctions, and integrin receptors by which endothelial cells adhere to each other and to extracellular matrix (ECM). *FN*: fibronectin, *VN*: vitronectin, *MMP's*: membrane metalloproteases, *Vin*: vinculin, *β*: β-catenin, *α*:α-catenin, *γ*: γ-catenin, *p120*: p120-catenin, *ZO*: zona occludin-1 protein, *JAM*: junctional adhesion molecule.

4.2.1.2 **Tight junctions**

Although AJs are the major components of endothelial junctions, TJs also play an important role in endothelial barrier function. About one-fifth of the endothelial cell junctions are TJs [44], and they consist of occludin and claudin, both of which form homotypic structures. The cell surface expression of occludin requires co-expression of its cytoplasmic binding protein zona occludin-1 (ZO-1) [45]. ZO-1 binds both cortical actin and occludins or claudins, and thereby links TJs to the actin cytoskeleton [38].

4.2.1.3 **Gap juctions**

GJs are intercellular channels formed by two connexons, one from each contributing cell, that create a 2-3 nm gap between the cells [46]. Connexon is a hexamer made of six connexin subunits [47]. Human umbilical vein endothelial cells express three different connexins: Cx37, Cx40, and Cx43 [48, 49] that are present in the intercellular channels in various compositions [38]. GJs transport information from cell to cell in form of second messengers (e.g. Ca^{2+} or IP_3) [50], and provide a low-resistance pathway for current flow, which allows changes in transmembrane potential to travel fast between the cells [51]. Communication between endothelial cells was implicated to play a role in initiating cell migration during formation of new capillary vessels, or when endothelial monolayer is repaired after vascular injury [52, 53]. Closing of the intercellular channels is regulated by phosphorylation of connexins, which disrupts gap junctional communication [54, 55]; however it is unclear how this affects endothelial barrier permeability [38]. Cx43 is linked to actin cytoskeleton via interaction with ZO-1 and spectrin, which may be important for regulation of endothelial barrier [38]. Based on studies in knock-out mice, connexins may play an important role in maintaining the integrity of the endothelial barrier. Double knock-out mice (*Cx37*$^{-/-}$, *Cx40*$^{-/-}$) displayed severe

vascular abnormalities and haemorrhaging in tissues, which led to prenatal death of the mice [56]. Endothelial cell specific Cx43 knock-out mice demonstrated elevated plasma NO levels and hypotension [57].

4.2.2 Signalling mechanisms regulating endothelial barrier permeability

The endothelial cell cytoskeleton is composed of actin microfilaments, intermediate filaments, and microtubules. The permeability of endothelial cell monolayer is highly dependent on actin microfilaments, while the roles of intermediate filaments and microtubules are not well defined [58]. The importance of actin microfilaments was demonstrated in cultured endothelial cells, where cytochalasin D, a known actin cytoskeleton disrupting agent, increased endothelial permeability [59]. In contrast the actin stabilizer phallacidin blocked the thrombin-induced increase in endothelial permeability [60]. Endothelial barrier permeability is regulated by chemical stimuli or by mechanical stress caused by blood flow [3]. Inflammatory mediators, such as thrombin, change the endothelial permeability by promoting endothelial cell shape change and contraction [38, 61], which is controlled by the dynamic rearrangement of actin cytoskeleton [58]. Thrombin increases endothelial permeability mainly by activating the G-protein-coupled proteinase-activated receptor-1 (PAR-1) [62], and deletion of PAR-1 receptor in mice abrogated the thrombin-induced increase in lung microvascular permeability [63]. The actin contractile machinery is also linked to many junction proteins, such as cadherins, zona occludens, zona adherens, and focal adhesion complex proteins [58], that contribute to the regulation of endothelial barrier.

Endothelial cell contraction is initiated by phosphorylation of the light chain of myosin II (MLC). The process is dually regulated by myosin light-chain kinase (MLCK) and myosin light-chain phosphatase (MLCP) (Figure 4). The rise in the intracellular Ca^{2+} concentration activates Ca^{2+}/calmodulin-dependent MLCK [64],

whereas the activation of RhoA/Rho kinase pathway leads to MLC phosphorylation by deactivating MLCP [65].

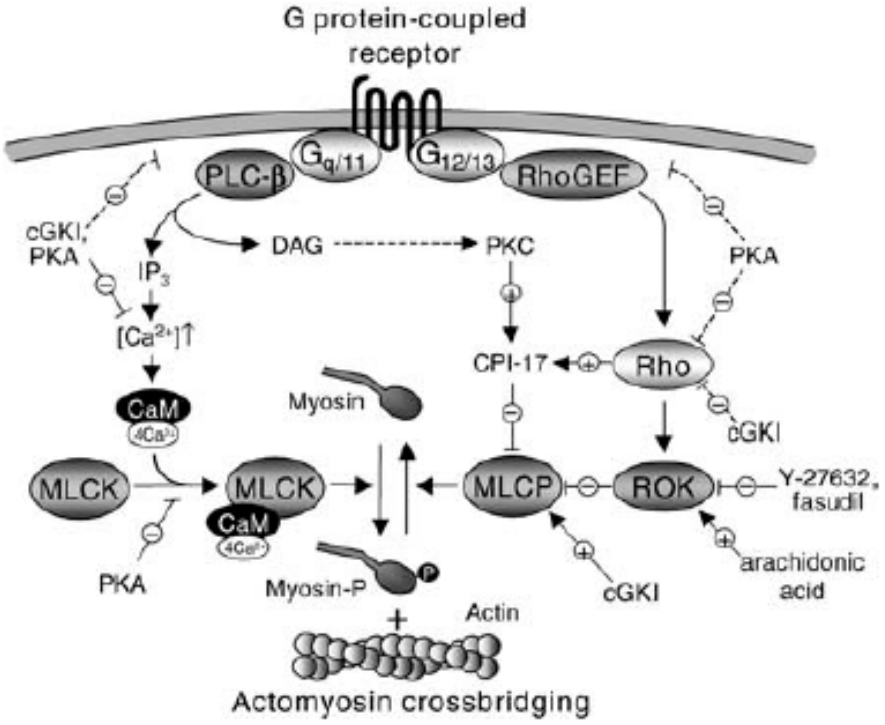

Figure 4. Dual regulation of myosin phosphorylation in smooth muscle and nonmuscle cells. MLC20 is phosphorylated by myosin light-chain kinase (*MLCK*) or myosin light-chain phosphatase (*MLCP*). *PLC*- β: β-isoforms of phospholipase C, *RhoGEF:* Rho-specific guanine nucleotide exchange factor, *IP3:* inositol-1,4,5-trisphosphate, *DAG*: diacylglycerol, *PKC:* protein kinase C, *CaM:* calmodulin, *ROK:* Rho-kinase, *cGK:* cGMP dependent kinase, *PKA:* cAMP-dependent kinase (protein kinase A). [66]

Under normal conditions the maintenance of endothelial cell integrity requires calcium (Ca^{2+}). The increase in intracellular Ca^{2+} concentration induces the opening of the endothelial barrier [58, 67-69]. Inflammatory mediators, such as thrombin, LPA, PAF, or histamine, induce increased endothelial permeability by causing shape change of endothelial cells, leading to retraction of the cells [63], and by disassembly of interendothelial junctions [70]. Binding of such a mediator to a G-protein-coupled receptor increases intracellular Ca^{2+} concentration by generation of inositol 1,4,5-triphosphate (IP_3), which activates IP_3 receptors on endoplasmic

reticulum. The increase in intracellular Ca^{2+} occurs in two phases. In the first phase Ca^{2+} is released from intracellular stores of endoplasmic reticulum, and in the second phase it enters the cell from extracellular space through plasma membrane channels [71, 72].

The increase in intracellular Ca^{2+} concentration activates Ca^{2+}/calmodulin-dependent myosin light chain kinase (MLCK) [64], and promotes disassembly of VE-cadherin at intercellular junctions [58, 69]. MLCK catalyzed phosphorylation of MLC was sufficient to induce endothelial cell contraction and dysfunction of the endothelial barrier [73]. Treatment of endothelial cells with MLCK inhibitors decreased endothelial barrier permeability produced by thrombin or histamine [61, 67]. Several studies suggest that also VE-cadherin regulates the permeability of endothelial barrier [74, 75] by Ca^{2+} dependent activation of PKC-α that mediates the disruption of VE-cadherin in adherens junctions. This was supported by the finding that thrombin-induced disorganisation of the VE-cadherin complex could be prevented by a PKC inhibitor calphostin C [76]. Thrombin-induced IP_3 formation stimulates the entry of Ca^{2+} via store-operated channels (SOC). TRPC4 (transient receptor potential channel 4) is a crucial constituent of the SOC in the mouse lung, and inhibition of Ca^{2+} entry via SOC by deletion of TRPC4 in mice reduced the thrombin-induced lung microvessel permeability by approximately 50 % [77].

Small GTPases, such as RhoA, regulate endothelial permeability by inducing MLC-dependent actin stress fiber formation and cell contraction [65]. Variety of stimuli acting through G-protein-coupled receptors activate Rho-GTPases [78]. Rho proteins are active when bound to GTP and inactive when bound to GDP [79]. Downstream of RhoA, Rho kinase (ROCK) phosphorylates the myosin binding subunit of MLCP and thus reduces its activity [80], leading to increased endothelial

permeability. ROCK is also known to phosphorylate occludin, and thereby disrupt TJs [81]. Thrombin-stimulated permeability increase could be blocked by treating endothelial cells with the specific RhoA inhibitor C3-transferase from *Clostridium botulinum* [82, 83], calcium chelators [67], or with Rho kinase inhibitor Y-27632 [84, 85].

In contrast to RhoA that increases endothelial barrier permeability, the small GTPases Rac1 and Cdc42 are known to destabilize the endothelial barrier [3]. However, in contrast to the barrier enhancing effects, Rac1 was shown to mediate the loss of endothelial barrier in response to VEGF and thrombin [86]. Recent data provided new information on the role of Rac1 in the disassembly of endothelial junctions upon VEGF stimulation [87]. The mechanism by which Rac1 activation disrupts endothelial barrier involves β-arrestin-dependent internalization of VE-cadherin. Cdc42 was demonstrated to be important for restoring the endothelial barrier after thrombin exposure [88]. Rac1 and Cdc42 get activated only after the RhoA activation subsides [89], suggesting that there is cross-talk between all these GTPases [3].

4.3 Role of endothelium in the regulation of vascular tone

4.3.1 Nitric oxide (NO)

In 1980 Furchgott and Zawadadzki discovered that endothelial cells released an unstable factor that was capable of relaxing blood vessels [90]. Later it was confirmed that this endothelium derived relaxing factor (EDRF) was nitric oxide (NO) [91-93]. Three different NO synthases (NOS) can produce NO, and they are named after the tissue where they were first found to be expressed: neuronal NOS (nNOS, *NOS1*), inducible NOS (iNOS, *NOS2*), and endothelial NOS (eNOS, *NOS3*) [94]. nNOS is constitutively expressed and involved in neurotransmission, whereas

iNOS is rapidly synthesized in response to inflammation [94]. Nitric oxide synthases oxidase L-argine to L-citrulline and NO [95], and regulate blood pressure, vascular remodelling and angiogenesis [96-98]. Continuous production of NO protects endothelium from atherogenesis [95] and is required for maintaining the endothelial barrier [99]. Several receptor-dependent agonists, such as acetylcholine or bradykinin, can stimulate NO release from endothelium. This mechanism is Ca^{2+} dependent, because chelation of extracellular Ca^{2+} or calmodulin (CaM) antagonist blocks NO production and relaxation of smooth muscle [100, 101]. Further downstream NO activates soluble guanylate cyclases (sGC) in vascular smooth muscle cells, thereby increasing cyclic GMP production [95]. Cyclic GMP can affect the vascular tone by for instance reducing the intracellular Ca^{2+} levels, or by activating protein kinase G [95]. Fluid shear stress stimulates the basal NO production independently of the increase in Ca^{2+} [102]. This so called "Ca^{2+} independent activation of eNOS" is regulated by Akt dependent phosphorylation of eNOS on Ser^{1177} [103, 104], but eNOS can also be phosphorylated on threonine and tyrosine residues [105]. Ser^{1177} is phosphorylated upon stimulation with thrombin [106], VEGF [103], bradykinin [107], or insulin [108], as well as under fluid shear stress condition [103]. In the basal state Ser^{1177} residue remains unphosphorylated. In contrast Thr^{495} is constitutively phosphorylated when unstimulated, and gets dephosphorylated when endothelium is stimulated with agonists that increase intracellular Ca^{2+}, such as histamine and bradykinin [95].

The role of eNOS in vascular homeostasis is essential. Mice lacking the endothelial nitric oxide synthase do not show acetylcholine-induced relaxation in vessels and are hypertensive [96, 109]. Endogenous NO negatively regulates vascular smooth muscle proliferation, and lack of it may cause abnormal remodelling and pathological changes in the morphology of vessel wall, associated with diseases like

hypertension and atherosclerosis [97]. Deficiency of eNOS led to impaired angiogenesis in a mouse model of hind limb ischemia [98]. NO is known to contribute to hypotension during LPS induced shock [110], and NO metabolites are found to be elevated in several animal shock models [111]. In addition, NO has a crucial role in anaphylactic shock as described later in 4.4.2.

4.3.2 Endothelium derived hyperpolarizing factor (EDHF)

Endothelium derived hyperpolarizing factor (EDHF) was discovered in the late eighties to be "the third" endothelial vasodilatating agent [112], in addition to the nitric oxide and prostacyclin systems [58]. EDHF received its name for its ability to hyperpolarize smooth muscle cells [113], which induces vasorelaxation by decreasing intracellular Ca^{2+}. To date it was not possible to identify a single molecule or pathway working as EDHF, and there are probably several EDHFs that can act alone, in parallel, or together [114]. Many different molecules and mediators have been proposed to act as EDHF in various tissues and species. There are reports showing the involvement of K^+ ions [115], cytochrome P450 metabolites [116, 117], lipoxygenase products [118], nitric oxide [119], reactive oxygen species (H_2O_2) [120], cAMP [121], C-type natriuretic peptide [122], and spreading of electronic current via myoendothelial gap junctions [123] in EDHF related vasodilation. It is currently unclear how these molecules and mediators regulate vasodilatation in different vascular beds.

NO, PGI_2, and EDHF contribute to vasodilatation in a different manner: NO system is more important in large diameter vessels, whereas EDHF contributes more to vasodilatation of small diameter vessels, and resistance sized arteries and arterioles [124]. Since these small diameter vessels and arteries control vascular tone and blood pressure [125], it is likely that EDHF has an important function in

regulating vascular homeostasis. For instance, EDHF is activated in essential hypertensive patients, indicating that EDHF may be a partial compensatory mechanism to maintain endothelium-dependent vasodilatation in hypertension, when NO availability is impaired [126]. It was also shown that EDHF was activated in cultured porcine coronary endothelial cells in response to cyclic stretch [127]. EDHF system was to be altered in different models of hypertension in rats [128, 129] and in diabetic rats [130].

There are increasing data of the contribution of EDHF to the blood pressure regulation from transgenic mice. Studies in endothelial NO synthase (eNOS) knock-out mice [96] and in eNOS and cyclooxygenase-1 (COX-1) double knock-out mice [131] suggested that EDHF was a major vasodilator in resistance vessels and could compensate for the loss of NO and PGI_2. This compensation was gender dependent: the resistance arteries of female eNOS/COX-1 knock-out mice preserved normal endothelium-dependent relaxations and mice were normotensive. In contrast the corresponding male mice suffered from hypertension and the relaxation of resistance arteries of these mice was impaired. This data suggested that EDHF plays a role in controlling arterial blood pressure, and may have a cardiovascular protective role in females.

4.4 Pathophysiology of endothelial cells

4.4.1 Inflammation

Vascular endothelium plays a key role in body's responses to infection, immune reactions, and tissue injury [132]. However, if uncontrolled, these normal defence mechanisms can contribute to numerous pathogenic disorders such as atherosclerosis, rheumatoid arthritis, ischemia/reperfusion injury, and allograft

rejection [132]. Endothelial barrier crucially regulates the leukocyte migration into the sites of inflammation [133]. The recruitment of leukocytes has been extensively studied using tools such as intravital microscopy, *in vitro* flow models, and genetic mouse models [132]. It is well established that recruitment of leukocytes is a multistep process: in the first step leukocytes start tethering and rolling, in the second step they firmly adhere to the endothelium, and in the third step leukocytes transmigrate into the tissue [134]. This process involves cytokine/chemokine signalling and leukocyte-endothelial interactions via various cell surface-expressed adhesion molecules [133] (Figure 5). The molecular mechanisms behind leukocyte rolling and adhering are fairly well understood, while the process of leukocyte transmigration is less clear at the molecular level [132].

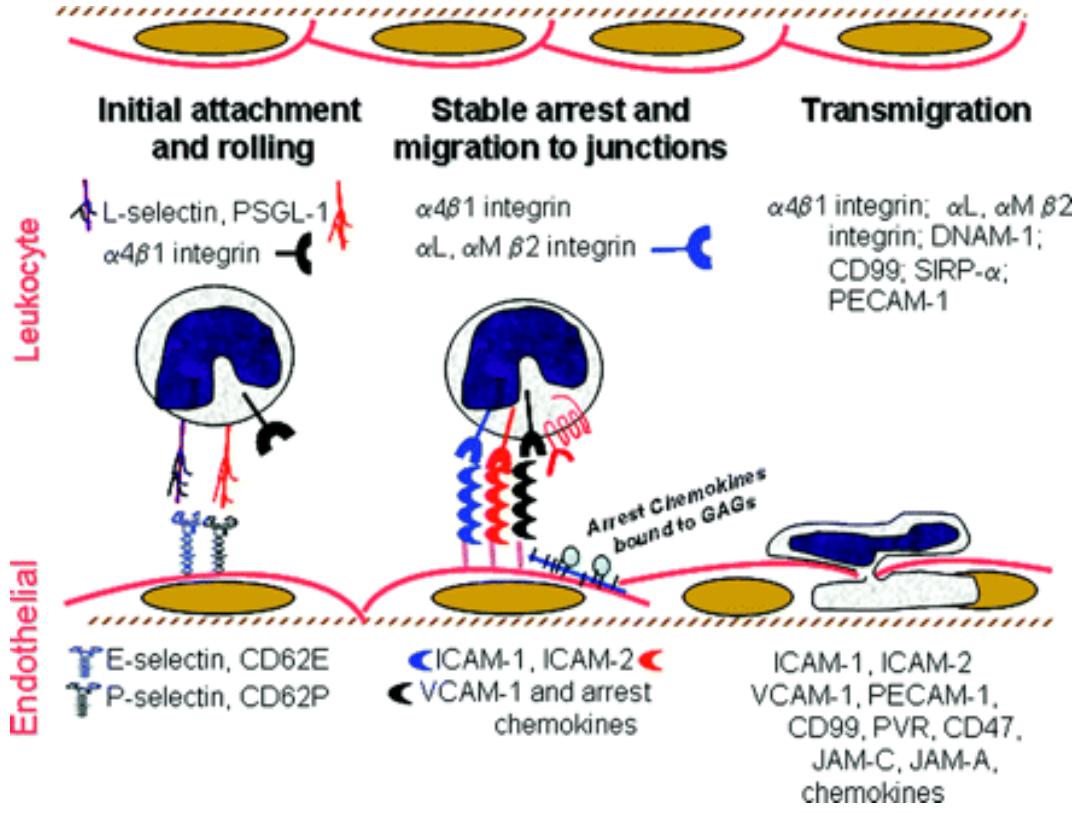

Figure 5. The multistep process of leukocyte recruitment [135]. Initial attachment, rolling, stable arrest, migration to the cell junctions, and transmigration of leukocytes across the endothelium. Shown are the adhesion molecules involved in each step.

The immune cells are first captured from circulation with help of endothelial selectins [134]. They mediate loose attachment of leukocytes to the endothelium and initiate leukocyte rolling, which is the first important step for leukocyte recruitment. In the venules of cremaster muscle, P-selectin supports tethering and rolling of leukocytes in the early phases of trauma-induced inflammation [136]. E-selectin is a mediator of slow rolling 2-4 h after tumour necrosis factor-α (TNF-α) injection [137], while L-selectin mediates tethering and rolling of leukocytes later after 6-8 hours in the TNF-α model [138]. P-selectin is stored in secretory granules called Weibel-Palade bodies, which are rapidly transported to the cell surface upon stimulation with inflammatory mediators histamine, thrombin, or TNF-α [139]. During acute inflammation P-selectin is the predominant receptor for leukocyte rolling in endothelial cells [139]. Deletion of P-selectin resulted in impaired rolling of leukocytes in murine venules *in vivo* [140, 141]. Same effects could be achieved by P-selectin antibody [140, 142] in rolling of human and murine leukocytes *in vitro* [143, 144], and in rolling of murine leukocytes *in vivo* [143, 145].

There is evidence that endothelial Ca^{2+} and RhoA signalling are involved in leukocyte recruitment. ICAM-1 cross-linking led to reorganisation of the actin cytoskeleton and activation of RhoA in rat brain endothelial cells [146, 147]. The transmigration of lymphocytes could be prevented by inhibiting RhoA [146]. Increase in endothelial cytosolic Ca^{2+} was shown to be involved in leukocyte migration across human umbilical vein endothelial cell monolayer [148]. Inhibition of endothelial MLCK activation significantly reduced leukocyte migration *in vitro* [61, 149, 150].

4.4.2 Anaphylactic shock

Anaphylactic shock is a severe and rapid, potentially fatal systemic allergic reaction characterised by hypotension, bronchospasm, utricaria, angioedema, and other symptoms [151]. Food, insect stings, or antibiotics can be the cause of anaphylactic reaction even when the patient has no history of allergy. The prevalence of anaphylactic shock is higher that generally thought, and it may affect 1-15 % of the population in the United States [152]. Severe pulmonary dysfunction and circulatory collapse often lead to death during anaphylactic shock and are resistant to the only currently available treatment: intravenous fluids, H_1-receptor antagonists, glucocotricoids, and adrenaline [151].

Anaphylactic reaction can be caused when an antibody (IgE) recognises an antigen, and crosslinked IgE binds to Fc receptors on basophils and mast cells leading to their degranulation. An alternative pathway involving IgG and macropages has also been described [153]. Several mediators are released from mast cells and basophils during anaphylactic reaction. These include histamine, tryptase, chymase, heparin, cytokines, prostaglandins, leukotrienes, and platelet activating factor (PAF) [151]. These mediators affect multiple organs during anaphylactic shock. PAF, histamine and tryptase induce vasodilation and capillary leakage by activating endothelial cells [154, 155]. PAF is considered to be a critical mediator of anaphylactic shock, since PAF antagonists or PAF-receptor deficiency are protective in animal models of anaphylactic shock [156, 157]. Vasodilator nitric oxide (NO) is generated during anaphylactic shock [91, 158, 159]. Anaphylaxis mediators bind to G-protein-coupled receptors on endothelial cells and activate signalling pathways leading to elevation of intracellular Ca^{2+} and production of NO. However, the source of NO in anaphylaxis has not been established, and the role of NO in anaphylaxis has been controversial; blocking of NO production was either beneficial or not [160-162].

Because cytokines can stimulate the expression of inducible iNOS, it has been generally considered that iNOS is the main mediator of anaphylactic shock and endotoxic shock [163, 164]. iNOS experession was upregulated in a mouse model of anaphylaxis in heart and lungs [165]. However, there are recent data showing that iNOS $^{-/-}$ mice were not protected from anaphylactic shock, while eNOS $^{-/-}$ mice were protected, indicating that anaphylactic shock depended on eNOS derived NO [159].

5 AIM OF THE STUDY

The endothelium has multiple physiological functions, and its dysfunction contributes to numerous human diseases. Mediators known to be involved in anaphylaxis and inflammation, such as histamine, PAF, and others, act through endothelial receptors coupled to various G-proteins including G_q/G_{11} and G_{12}/G_{13}. However, the contribution of individual G-protein mediated signalling pathways to the regulation of endothelial functions *in vivo* is unclear. To investigate the role of G-protein mediated signalling pathways in the adult endothelium, we generated endothelial cell specific double knock-out mice for the genes encoding the α-subunits of G_q/G_{11} and G_{12}/G_{13} using the Cre/LoxP system. The aim of this study was to elucidate the role of G-protein mediated signalling involved in the regulation of endothelial functions both under physiological and pathophysiological conditions.

6 MATERIAL AND METHODS

6.1 Reagents

Acetic acid	Merck, Darmstadt
Agarose	Carl Roth, Karlsruhe
Albumin, human-dinitrophenyl	Sigma, Deisenhofen
Ammonium acetate	Carl Roth, Karlsruhe
APS, ammonium peroxidisulfate	Carl Roth, Karlsruhe
Bromophenol blue sodiumsalt	Sigma, Deisenhofen
BSA, bovine serum albumin	Sigma, Deisenhofen
BSA, bovine serum albumin, 30 % solution	PAA Laboratories GmbH, Cölbe
Calcium chloride	Merck, Darmstadt
Dil-Ac-LDL (human low density lipoprotein)	Tebu-Bio, Offenbach
Dispase	BD Biosciences, Heidelberg
DMEM/F12	Invitrogen, Karlsruhe
Dynabeads® Sheep anti-Rat IgG	Invitrogen, Karlsruhe
EDTA, disodium ethylenediaminetetra-acetate	Merck, Darmstadt
EGTA, ethylenedioxy-bis-(ethylenenitrilo) tetra acetic acid	AppliChem, Darmstadt
Endothelial cell growth supplement with heparin	Promocell, Heidelberg
Eosin, Y solution	Medite, Burgdorf
Ethanol absolute	AppliChem, Darmstad
Ethidium bromide	Merck, Darmstadt
Evans Blue	Sigma, Deisenhofen
Fibronectin, human	BD Pharmingen, Heidelberg
Foetal bovine serum	Invitrogen, Karlsruhe

Formamide	Sigma, Deisenhofen
Giemsa stain	Merck, Darmstadt
Glutardialdehyde solution, 25%	Merck, Darmstadt
Glycerol, 1,2,3-propanetriol	Merck, Darmstadt
Glycine	Riedel-de Haën, Deisenhofen
HBSS, Hank's balanced salt solution	Invitrogen, Karlsruhe
Histamine dihydrochloride	Sigma, Deisenhofen
IBMX, 3 isobutyl-1-methylxanthine	Applichem, Darmstadt
Ionomycin	Invitrogen, Karlsruhe
Isopropanol, 2-propanol	AppliChem, Darmstad
Ketanest® ketamine	Parke-Davis, USA
L-NAME (N_ω-Nitro-L-arginine methyl ester hydrochloride)	Sigma, Deisenhofen
Lysophosphatic acid	Sigma, Deisenhofen
Magnesium chloride	Merck, Darmstadt
Magnesium sulfate	Merck, Darmstadt
β-2-mercaptoethanol	Merck, Darmstadt
Methanol	Merck, Darmstadt
Miglyol	Pharmacy, University of Heidelberg
Milk, nonfat dry	AppliChem, Darmstad
Mineral oil	Sigma, Deisenhofen
Mowiol® 4-88	Calbiochem/Merck, Schwalbach
Narcoren®, 16% (Pentobarbital sodium salt)	Merial, Hallbergmoos
Normal goat serum	Vector, Wertheim-Bettingen
NP-40, Nonidet® P40, nonylphenyl-polyethylene glycol	AppliChem, Darmstad
dNTP-Set, 2'-deoxynucleoside 5'-triphosphate	Carl Roth, Karlsruhe

O.C.T. freezing medium	Leica Microsystems, Nussloch
PAR-1 peptide (Ser-Phe-Leu-Leu-Arg-Asn-amide)	Sigma, Deisenhofen
Paraformaldehyde	Riedel-de Haën, Deisenhofen
PBS	Invitrogen, Karlsruhe
Pertex®	Medite, Burgdorf
Pertussis toxin	Calbiochem/Merck, Schwalbach
Penicillin-streptomycin	Invitrogen, Karlsruhe
Phenol Red	AppliChem, Darmstad
Platelet activating factor (PAF)	Sigma, Deisenhofen
Ponceau S, 2,7-naphthalene disulfonic acid	AppliChem, Darmstad
Potassium chloride	Merck, Darmstadt
Potassium dihydrogen phosphate	AppliChem, Darmstad
Potassium hexacyanoferrate II	Merck, Darmstadt
Potassium hexacyanoferrate III	Riedel-de Haën, Deisenhofen
Proteinase K from *Tritirachium album*	AppliChem, Darmstad
Rompun®, 2% (Xylazin chydrochlorid)	Bayer Vital, Leverkusen
Rotiphorese® Gel 30	Carl Roth, Karlsruhe
SDS, sodium dodecyl sulfate	Fluka, Deisenhofen
Sodium azide	Merck, Darmstadt
Sodium chloride	AppliChem, Darmstad
Sodium deoxycholate	AppliChem, Darmstad
Sodium dihydrogen phosphate	Riedel-de Haën, Deisenhofen
di-Sodium hydrogen phosphate	Riedel-de Haën, Deisenhofen
Sodium hydroxide	Carl Roth, Karlsruhe
Sodium hydrogen carbonate	Ferak, Berlin
Sodium nitroprusside (SNP)	Sigma, Deisenhofen

Sucrose	J.T.Baker, Deventer
Superoxide dismutase	Roche, Mannheim
Tamoxifen	Sigma, Deisenhofen
TEMED	AppliChem, Darmstad
Thrombin	Sigma, Deisenhofen
Trichloroacetic acid	Merck, Darmstadt
Tris, tris-(hydroxymethyl)-aminomethan	Carl Roth, Karlsruhe
Triton X-100, octylphenoxypolyethoxyethanol	Merck, Darmstadt
Trypsin-EDTA	Invitrogen, Karlsruhe
Tween-20	AppliChem, Darmstad
Tyrode's salt	Sigma, Deisenhofen
X-Gal, 5-bromo-4-chloro-3-indolyβ-D-galactopyranoside	AppliChem, Darmstad
Xylene	Merck, Darmstadt
Xylene cyanol FF	AppliChem, Darmstad
SmartLadder™	Eurogentec, Köln
PageRuler™ Prestained Protein Ladder	Fermentas, Heidelberg

6.2 Antibodies

Rabbit anti-mouse $G\alpha_{13}$, polyclonal	Santa Cruz, Heidelberg
Rabbit anti-mouse $G\alpha_{q/11}$, polyclonal	Santa Cruz, Heidelberg
Mouse anti-mouse α-tubulin, monoclonal	Sigma, Deisenhofen
Rabbit anti-mouse pMLC, monoclonal	New England Biolabs GmbH, Frankfurt
Mouse anti-mouse MLC, monoclonal	Sigma, Deisenhofen
Goat anti-rabbit IgG, horseradish peroxidase-conjugated	Sigma, Deisenhofen
Sheep anti-mouse IgG, horseradish peroxidase-conjugated	Amersham, Freiburg
Mouse monoclonal anti-DNP-HSA IgE	Sigma, Deisenhofen
Rat anti-mouse CD144 (VE-Cadherin)	BD Pharmingen, Heidelberg
Rat anti-mouse RB40 (P-selectin)	BD Pharmingen,Heidelberg

6.3 Kits

Amersham D-myo-Inositol 1,4,5-triphosphate (IP_3) [^{3}H] Biotrak assay system	GE Healthcare Buchler GmbH, Braunschweig
ECL Western Blotting System	Amersham Pharmacia, Heidelberg
G-LISA^{TM} RhoA activation assay biochem kit^{TM}	Tebubio, Offenbach
cGMP radioimmunoassay	GE Healthcare Buchler GmbH, Braunschweig

6.4 Buffers and solutions

Buffers and solutions were prepared in fresh double-distilled and deionised water.

Table 1.

Buffer name	**Components**	**Final concentration**	**Remarks**
Blocking solution	Tris-HCl NaCl BSA Phenol-red NaN_3	20 mM 350 mM 5% 0.005% 0.1%	pH 7.5
β-galactosidase basic buffer	NaH_2PO_4 Na_2HPO_4 EGTA $MgCl_2$	23 mM 77 mM 5 mM 2 mM	pH 7.3
β-galactosidase fixing buffer	NaH_2PO_4 Na_2HPO_4 EGTA $MgCl_2$ glutaraldehyde	23 mM 77 mM 5 mM 2 mM 0.2%	pH 7.3
β-galactosidase washing buffer	NaH_2PO_4 Na_2HPO_4 EGTA $MgCl_2$ sodium deoxycholate NP-40	23 mM 77 mM 5 mM 2 mM 0.01% 0.02%	pH 7.3

Buffer name	Components	Final concentration	Remarks
β-galactosidase staining buffer	NaH_2PO_4 Na_2HPO_4 EGTA $MgCl_2$ sodium deoxycholate NP-40 potassium hexacyanoferrate II potassium hexacyanoferrate III X-Gal	23 mM 77 mM 5 mM 2 mM 0.01% 0.02% 10 mM 10 mM 0.5 mg/ml	pH 7.3
Bicarbonate buffer	NaCl KCl $CaCl_2$ $MgCl_2$ $NaHCO_2$	125 mM 4.5 mM 2 mM 1 mM 17 mM	
Mowiol®	Mowiol® 4-88 Glycerol TrisHCl	10% w/v 25 % w/v 0.1M	 PH 8.5
Paraformaldehyde (4% PFA)	PFA PBS	4% w/v	PH 8.0
PCR buffer	Tris-HCl pH 8.4 KCl	200 mM 500 mM	
PBS	Na_2HPO_4 KH_2PO_4 NaCl KCl	8 mM 1.5 mM 137 mM 2.7 mM	pH 7.4
Ponceau S	Ponceau S Glacial acetic acid	0.2% 1%	
Sample buffer (6×) (Agarose gels)	Bromo phenol blue Xylene Cyanol Glycerol	0.25% 0.25% 30%	

Buffer name	Components	Final concentration	Remarks
Sample buffer (4×) (Protein gels)	TrisHCl SDS Glycerol Bromo phenol blue 2-Mercaptoethanol	0.28 M 6% 20% 0.28 g/ml 3%	pH 6.8
SDS running buffer(10×)	TrisHCl Glycine SDS	0.25 M 1.92 M 1 M	pH 8.3
SDS separating gel buffer	Tris base SDS	0.75 M 0.2%	pH 8.8
SDS stacking gel buffer	Tris base SDS	0.25 M 0.2%	pH 6.8
TAE buffer (50×)	Tris base Glacial acetic acid EDTA	242 g/l 57.1 ml 37. 2 g/l	pH 8.0 pH 8.0
Tail lysis buffer	EDTA TrisHCl SDS Proteinase K	100 mM 50 mM 0.5% 0.5 mg/ml	pH 8.0
TBS	TrisHCl NaCl	10 mM 150 mM	pH 7.5
TBST	TBS Tween-20	1× 0.05%	
Transfer buffer	Tris base Glycin SDS Methanol	25 mM 192 mM 0,01% 10	
Tyrode buffer	Tyrode's salt Hepes	 10 mM	pH 7.3-7.4

6.5 Breeding and genotyping of mice

Maintaining and breeding of mutant mice and experiments were performed in appropriate rooms at the Central Animal House of the University of Heidelberg, and conducted according to the Experimental Animals Care and Use Law from 25 May 1998.

6.5.1 Isolation of the genomic DNA

The genomic DNA was isolated and purified from tail biopsies that were digested overnight in 300 µl of tail lysis buffer at 56°C with vigorous shaking, and centrifuged at 13000 rpm to remove impurities. In order to precipitate the DNA, 200 µl of supernatant was transferred into a fresh test tube containing 100 µl of 7.5 M ammonium acetate and 600 µl ice cold 100% EtOH, and incubated at -20°C for 10 minutes. Precipitated DNA pellet was washed once in 70% EtOH and shortly dried at 37°C. DNA was dissolved in 200 µl of sterile water for 1 hour at 37°C, 1000 rpm.

6.5.2 Genotyping of mice by polymerase chain reaction (PCR)

Tie2-Cre transgenic mice were kindly provided by Dr. Schütz (DKFZ, Heidelberg). $G\alpha_q^{flox/flox};G\alpha_{11}^{-/-}$ as well as $G\alpha_{13}^{flox/flox};G\alpha_{12}^{-/-}$ mutant animals were generated as previously described [17, 18, 34, 166]. Rosa26-LacZ mice were obtained from The Jackson Laboratory (Bar Harbor, M.E., USA). The generation of the reporter Rosa26-LacZ mouse line has been described [167].

The PCR mixture was prepared on ice in PCR buffer and contained the indicated $MgCl_2$ concentration, dNTP-Set (25 mM), each required primer (50 µmol), and *Taq* DNA polymerase (1.25 U) in a final volume of 50 µl per sample. The reagents were overlaid with 100 µl of mineral oil to prevent evaporation during the thermal cycling process. The PCR was run using thermocycler (PTC-200, MJ Research/BioRad, München). The PCR-programs and primers used for each PCR are described in the Table 2.

Table 2.

Allele	Primers and amplification products	PCR parameters
Tie2-Cre	5'-GAAGTCGCAAAGTTGTGAGTTG-3' 5'-TGGCTTGCAGGTACAGGAG-3' 5'-GAGAATGGCGAGAAGTCACTG-3' 207 bp amplification product for the wild type allele and 331 bp for the transgenic allele	2.5 mM MgCl 4 min at 94°C 35 cycles: 30 sec at 94°C 30 sec at 58°C 1 min at 72°C 5 min at 72°C
Rosa26-lac-Z	5'-AAAGTCGCTCTGAGTTGTTAT-3' 5'-GCGAAGAGTTTGTCCTCAACC-3' 5'-GGAGCGGGAGAAATGGATATG-3' 500 bp amplification product for the wild type allele and 250 bp for the transgenic allele	1.5 mM MgCl 3 min at 94°C 29 cycles: 30 sec at 94°C 30 sec at 58°C 45 sec at 72°C 10 min at 72°C
Gnaq *Gnaq*^{fl}	5´-AGCTTAGTCTGGTGACAGAAGC-3´ 5´-GCATGCGTGTCCTTTATGTGAG-3´ amplification products with 600 bp for the wild type allele and 700 bp for the mutant allele	1.5 mM MgCl 3 min at 94°C 30 cycles: 20 sec at 94°C 20 sec at 60.5°C 135 sec at 72°C 10 min at 72°C
Gna11^{+}	5´-GCCCCTTGTACAGATGGCAG-3´ 5´-AGCATGCTGTAAGACCGTAG-3´ amplification product with 820 bp for the wild type allele	1.5 mM MgCl 3 min at 94°C 30 cycles: 30 sec at 94°C 30 sec at 64°C 90 sec at 72°C 10 min at 72°C

Gnα11^{-}	5′-CAGGGGTAGGTGATGATTGTGC-3′ 5′-GACTAGTGAGACGTGCTACTTCC-3′ amplification product with 250 bp for the mutant (null) allele	1.5 mM MgCl 3 min at 94°C 30 cycles: 30 sec at 94°C 30 sec at 57°C 120 sec at 72°C 10 min at 72°C
Gnα13^{fl}	5′-GCACTCTTACAGACTCCCAC-3′ 5′-GCCACAGAGGGATTCAGCAC-3′ amplification products with 420 bp for the wild type allele and 500 bp for the mutant allele	1.7 mM MgCl 5 min at 95°C 40 cycles: 15 sec at 95°C 15 sec at 56°C 150 sec at 72°C 10 min at 72°C
Gnα12^{+} *Gnα12*$^{-}$	5′-GTGCTCATCCTTCCTGGTTTCC-3′ 5′-CGGGTCGCCCTTGAAATCTGG-3′ 5′-GGCTGCTAAAGCGCATGCTCC-3′ amplification products with 440 bp for the wild type allele and 310 bp for the mutant (null) allele	1.7 mM MgCl 5 min at 94°C 36 cycles: 60 sec at 94°C 60 sec at 65°C 120 sec at 72°C 10 min at 72°C

6.5.3 Agarose gel electrophoresis

To separate DNA fragments that were amplified in PCR, 1% agarose gel in TAE buffer with 10 µg/ml ethidium bromide was used. Electrophoresis of DNA fragments in agarose gel was performed in horizontal chamber (Biometra, Göttingen) in TAE buffer. DNA molecular weight standard and 25 µl of samples obtained as described containing 1x sample buffer were loaded into the wells of the gel. Electrophoresis was conducted at constant 200 mA amperage and at 10 V per cm of gel length voltage. Results of separation were registered by the GelDoc System (BioRad, München), where the gel was illuminated with UV light and visualized by the Quantity One v.4.2.1 software module.

6.6 Histology and detection of β-galactosidase activity

To verify inducibility and activity of the Cre fusion protein, *tie2-Cre*ER^{T2} mice were mated with the mice from Cre-reporter transgenic line, Gt(ROSA)26Sortm1sor (ROSA26-LacZ). Tie2$^{+/-}$, ROSA-26-LacZ$^{+/-}$ offspring from these matings were treated with tamoxifen (5 x 1 mg/d i.p.) or vehicle alone and were sacrificed 14 d after beginning of induction. The expression of Tie2-promoter driven recombination was analyzed by detection of β-galactosidase activity.

6.6.1 Preparation of tissues for cryosectioning

The mice were anesthetised with pentobarbital sodium (50 mg/kg) and perfused with PBS and 0.2 % PFA. Organs were removed and fixed overnight in 0.2% paraformaldehyde solution at 4^{o}C. Next day organs were soaked overnight in 30 % sucrose solution at 4^{o}C. Afterwards organs were embedded in O.C.T. freezing medium, frozen on dry ice and serially sectioned at 10-15 µm thickness on a cryostat (CM 3050 S, Leica, Nussloch). Sections were placed onto gelatine-coated Star Frost® microscope slides (Medite, Burgdorf) and processed according to X-Gal staining protocol.

6.6.2 X-Gal staining of cryosections

Cryosections were fixed in β-galactosidase fixing buffer for 5 minutes at room temperature and washed three times 5 minutes on ice with β-galactosidase washing buffer. Subsequently, sections were stained overnight in β-galactosidase staining buffer at 37°C and rinsed shortly in PBS to remove rests of staining buffer. Slides were counterstained with eosin for 2 minutes. In order to remove excess eosin and to preserve sections, slides were rinsed in 0.01% acetic acid and dehydrated through ethanol series (70% and 80% for 20 seconds each, and 95% and absolute for 2 minutes each). After dehydration slides were immersed two

times in xylene for 5 minutes, mounted in a quick hardening mounting medium (Pertex®) using covering glasses (Medite, Burgdorf) and viewed under the light microscope (MZ FL III, Leica, Nussloch) equipped with a digital camera (Coolpix 4500, Nikon, Düsseldorf).

6.7 Detection of protein expression by Western blotting

6.7.1 SDS-polyacrylamide gel electrophoresis

SDS-polyacrylamide gel electrophoresis was performed to separate proteins. Mini-Protean III system (BioRad, München) with a 1 mm thick gel sandwich was used for electrophoresis. The SDS percentage of the separating gel was chosen according to the size of protein of interest. 10% gels were used for G-proteins α-subunits, and 12% gels were used for pMLC and MLC. The gel was covered with isopropanol and allowed to polymerise at room temperature. In order to concentrate isolated proteins, 6% SDS-stacking gel was prepared on top of separating gel. After complete polymerisation, gels were assembled in the vertical electrophoresis chamber. Protein electrophoresis was done in electrode buffer with 5 µl of protein molecular weight standard and samples obtained as described. Electrophoresis was conducted at 145 V until the desired separation of the protein of interest was achieved. Afterwards, gels were subjected to electrotransfer.

6.7.2 Protein electrotransfer

Proteins were transferred from the SDS-polyacrylamide gel onto a nitrocellulose membrane (Protran®, 0.45 µm, Schleicher & Schuell, Dassel) using a Mini-Trans-Blot system (BioRad, München). Electrotransfer was performed in transfer buffer and conducted at 350 mA for 1 hour. In order to determine the efficiency of transfer and equality of loading, membranes were shortly stained in Ponceau S staining solution. After washing with TBS-TW the membrane was incubated in blocking

solution for 1 hour. The membrane was incubated with the primary antibody overnight at 4^{o}C, washed three times 10 minutes with TBS-TW, and incubated with a specific horseradish peroxidase-conjugated secondary antibody in 5 % dry milk in TBS-TW for 1 hour. The membrane was washed again three times for 10 minutes in TBS-TW, immunoreactive bands were visualized through the enhanced chemiluminescence (ECL) detection system, and the result was registered on the X-ray film (Kodak® X-Omat AR, Sigma, Deisenhofen). The film was developed in a X-ray film processor (Optimax, Protec, Oberstenfeld).

Primary antibodies used for immunodetection were diluted 1:200 for anti-G$\alpha_{q/11}$ and anti-Gα_{13}, 1:5000 for anti-α-tubulin, 1:1000 for pMLC, and 1:200 for MLC antibody. Secondary antibodies were diluted 1:1000 for horseradish peroxidase-conjugated anti-rabbit IgG and 1:5000 for horseradish peroxidase-conjugated anti-mouse IgG antibody.

6.8 Mouse primary endothelial cell isolation and culture

6.8.1 Coating of magnetic beads

Magnetic beads (Dynabeads M450, sheep anti-rat IgG) were carefully resuspended and required amount transferred into an eppendorff tube. Beads were washed with 1 ml of PBS/0.5% BSA and recovered with Dynabead magnet. Washing step was repeated 3 times and beads were resuspended in their original volume. In order to purify endothelial cells, 2.5 µg of anti-mouse CD144 antibody was used for coating 25 µl of beads. Beads and antibody were incubated in an overhead rotating mixer for 1 hour at room temperature. After incubation beads were washed 3-4 times as described before and used for magnetic purification of endothelial cells. Coating was always performed in parallel to cell preparation and coated beads were stored for maximum 1 hour.

6.8.2 Isolation of endothelial cells

Mouse pulmonary endothelial cells were isolated as previously described [168]. Mice were sacrificed by cervical dislocation and lungs from 2-4 mice per genotype were collected in PBS on ice. Lung tissue was minced to 1 mm sized pieces with sterile scissors and minced tissue was washed in PBS with help of a 70 µm mesh cell sieve (BD Falcon). The tissue was further transferred into 20 ml of dispase solution (4.5-5.0 U/ml in HBSS). Lung tissue was digested at 37°C with shaking (250 rpm) for 1 hour. To further reduce the size of cell aggregates tissue was pipetted several times up and down with a 5 ml pipette. Tissue was then filtered through a 70 µm mesh cell sieve into a falcon tube containing 20 ml PBS/10% FBS. Cells were recovered by centrifugation at 1200 rpm for 5 minutes and washed twice with 10 ml of PBS/0.5% BSA. The cell pellet was resuspended in 350-700 µl of PBS/0.5% BSA and incubated with coated beads in an overhead rotating mixer for 30 minutes at room temperature. Before recovering cells with the magnet, cells were filtered through a 30 µm sieve in order to reduce the size of cell aggregates. Cells were washed 2-3 times with PBS/0.5% BSA and seeded on fibronectin coated 24-well plates. Endothelial cells were cultured in DMEM/F12 supplemented with 10% FBS, penicillin/streptomycin (100 U/ml, 100 mg/ml), and endothelial cell growth supplement/heparin at 37°C, 5% CO_2. In order to induce Cre-mediated recombination, the cells were infected with 5×10^7 PFU of Adeno-Cre-GFP-virus (Vector Biolabs) 72 hours prior to the experiments.

6.8.3 Purification of primary endothelial cell cultures

Primary cultures contained small amounts of other cells types that had adhered endothelial cells during isolation, therefore the primary cultures were purified if necessary at passage 1. Beads were coated as described in. 3 µl of coated beads was used per 24-well of cells. Cells were washed twice with PBS/0.5% BSA before

the beads were added on cells. Incubation of beads was carried out for 1 hour. At 30 min plates were gently shaked to resuspend non-attached beads. Cells were washed twice with PBS/0.5% BSA, and incubated with trypsin for 3 minutes at room temperature. Detached cells were washed and centrifuged 1200 rpm for 5 minutes. Cells were recovered with magnet and seeded on fibronectin coated dishes. Purity of endothelial cells was determined by uptake of fluorescently labelled LDL (Tebu-Bio). Cells were incubated with 10 µg/ml of Dil-Ac-LDL for 4 hours, washed, and fixed with 4% PFA. Nuclei were stained with Dapi and coverslips mounted with Mowiol.

6.8.4 Immunofluorescence staining of primary endothelial cells

The purity of freshly isolated mouse primary pulmonary endothelial cells was analyzed by immunofluorescence staining with CD144 antibody (VE-cadherin, BD Pharmingen). Briefly, the cells were cultured on fibronectin coated coverslips and fixed with 4% PFA for 10 minutes at room temperature. The cells were permeabilized with PSB/0.5% Triton-X-100 for 5 minutes at room temperature, washed twice in PBS and then blocked with 10% goat serum in PBS for 1 hour at room temperature. The cells were incubated with anti-CD144 antibody (1:200) o/n at 4°C. Next day the cells were washed 3 times in PBS before incubation with anti-rat-TRITC secondary antibody for 1 hour at room temperature, washed again, and coverslips mounted with Moviol. Stained cells were observed with a fluorescent microscope (Leica DM IRE2, Leica Microsystems, Wetzlar) and photos taken with a camera (Leica DC 350F, Leica Microsystems, Wetzlar).

6.9 *In vitro* experiments

6.9.1 Inositol 1,4,5-triphosphate (IP_3) assay

Inositol 1,4,5-triphosphate (IP_3) production on primary endothelial cells was determined by a radioactive D-*myo*-Inositol 1,4,5-triphosphate (IP_3) [$_3$H] Biotrak assay system (Amersham). The assay was based on competition between the radioactive tracer ([$_3$H] IP_3) and unlabelled IP_3 in the standard or samples for binding to a binding protein prepared from bovine adrenal cortex.

For inducing IP_3 production cells were stimulated with 1 u/ml thrombin for 15 seconds. Stimulation was stopped by adding equal volume of ice-cold 15% trichloroacetic acid (TCA) to extract proteins. Cells were scratched and precipitates were sedimented by centrifugation at 2000 x g for 15 minutes at 4°C. IP_3 containing supernatant was washed three times with 10 volumes of water-saturated diethyl ether. Samples were stored at –20°C and neutralized to pH 7.5 with $NaHCO_3$ just before starting the experiment.

Prior starting IP_3 assay standards (0.19-25 pmol IP_3) were prepared by dilution from standard stock. Polypropylene tubes were labelled as duplicates for samples and controls and 100 µl of assay buffer was pipetted into tubes. After addition of assay buffer 100 µl of each standard and sample were added. For determining B_0 100 µl of water was added into B_0 tubes, and for measuring total count 200 µl of water was pipetted into TC tubes. For determining non-specific binding 100 µl of stock standard was added into NSB tubes. Diluted tracer (100 µl) was added into all tubes and binding protein (100 µl) into all tubes except TC. Tubes were vortex mixed and incubated on ice for 15 minutes. The bound IP_3 was separated from the free IP_3 by centrifugation at 2000 x g for 10 minutes at 4°C. TC tube was not centrifuged. After

centrifugation supernatant was discarded and the rests of liquid removed from tubes by wiping inside of the tubes with absorbent tissues. Pellets were resuspended in 1 ml of 0.15 M NaOH and incubated at RT for 10 minutes. Samples were neutralized with 50 µl of 10% acetic acid and decanted into scintillation vials. Radioactivity of the samples was measured with a gamma counter. The amount of unlabelled IP_3 in the sample was determined by interpolation from a standard curve.

6.9.2 RhoA activation assay

RhoA activation on primary endothelial cells was detected by a luminescence based G-LISA™ RhoA activation assay kit (Tebubio). Cell material needed for this assay was 10-50 µg/assay (12-well plate) and detection limit of the assay was 0.025 ng RhoA.

A day before the experiment cells were starved in medium containing 0.5% FBS o/n. On the day of experiment cell were cultured 3-4 hours without FBS.

In order to activate RhoA, cells were stimulated with 1 u/ml thrombin for 1 minute, then washed with 1.5 ml ice-cold PBS and lysed in 150 µl of lysis buffer containing proteinase inhibitor (1:1000) provided by the kit on ice. Immediately after lysing samples were spinned down at 13000 rpm, 4°C. For protein measurement and Western blot 20 µl of supernatants were transferred into new Eppendorf tubes, and 60 µl of supernatant was frozen in liquid nitrogen. Protein concentrations were measured by spectroscopy (BioPhotometer, Eppendorf-Netheler-Hinz GmbH, Hamburg, Germany) and equalized with lysis buffer if necessary. Lysates were then thawed in waterbath at room temperature and equal volume of binding buffer was added to them. A volume of 50 µl of lysate was pipetted as duplicates on RhoA

affinity wells. Lysis buffer was used as buffer blank control and RhoA control protein was used as positive control. Affinity plate was shaken at 400 rpm at 4°C for 30 minutes. Plate was then washed 2 times with washing buffer and incubated with 200 µl antibody presenting buffer for 2 minutes at room temperature, following 3 additional washes. RhoA antibody (1:500) was added on wells and plate was shaken at 400 rpm at room temperature for 45 minutes. After primary antibody incubation plate was washed 3 times and incubated with secondary antibody (1:1000) for 45 minutes (400 rpm). Wells were washed 3 times with washing buffer and HRP detection reagent was added on them. Luminescence signal was read immediately using a microplate luminometer (Luminoscan Ascent, Labsystems, Thermo Electron Corporation, Dreieich, Germany). Results were expressed as fold stimulation over basal.

6.9.3 Detection of MLC phosphorylation in endothelial cells by Western blot

The cells were starved o/n in medium containing 0.5% FBS. The next day cells were stimulated with 1 u/ml thrombin for 1, 3, or 10 min, lysed with 2 x Läemmli, boiled for 10 minutes at 100°C, and centrifuged 13000 rpm for 10 minutes before the samples were loaded on 12% SDS PAGE gel. MLC phosphorylation was detected by anti-p-MLC antibody.

6.9.4 Determination of NO production

The NO production was determined as previously described [169]. Cultured lung endothelial cells from wild-type, $G\alpha_q^{fl/fl}$, $G\alpha_{11}^{-/-}$, or $G\alpha_{13}^{fl/fl}$, $G\alpha_{12}^{-/-}$ mice were suspended by treatment with accutase and washed in HEPES-buffered Tyrode solution containing the phosphodiesterase inhibitor 3 isobutyl-1-methylxanthine (IBMX, 0.1 mmol/L) and superoxide dismutase (100 U/mL). Approximately 5×10^4 cells were added to RFL6 fibroblasts cultured in 24-well plates, and

incubated (37°C) in the absence or presence of PAF (100 nmol/L, 5 minutes), thrombin (1 u/ml, 5 minutes), or ionomycin (100 nmol/L, 2 minutes). Thereafter, the incubation was stopped by the addition of trichloroacetic acid (6%) and the concentration of cyclic GMP was determined by a radioimmunoassay.

6.10 *In vivo* experiments

6.10.1 Vascular permeability assay *in vivo*

Vascular permeability assay was performed using Evans blue dye. Evans blue binds to plasma proteins and remains in the vasculature unless the vascular permeability changes [170]. Vascular permeability can thus be determined by evaluating the Evans blue content in the tissue. Mice were anesthetised with pentobarbital sodium (50 mg/kg). They received an i.v. injection of Evans Blue in saline (0.04 µg/g). After 1 minute, mice were injected with different concentrations of agonists in 20 µl of PBS into the shaved back skin. PBS was injected as control. Mice were kept on a heating plate at 37°C for 10 minutes before they were sacrificed by cervical dislocation, and approximately 1 cm^2 pieces of skin containing the injection site were removed. The skin pieces were incubated in 500 µl of formamide at 55°C for 48 hours, and the Evans blue content was determined by absorption at 595 nm with spectrophotometer (Multiscan Ascent, Labsystems, Thermo Electron Corporation, Dreieich, Germany).

6.10.2 Passive cutaneous anaphylaxis

Control and knock-out mice were injected with 30 ng of anti-DNP-HSA IgE in 20 µl of sterile 0.9% NaCl into the dorsal skin of the right ear. The left ear of mice received equal volume of saline and served as control. After 24 hours passively immunized mice were challenged by an i.v. injection of 0.5 mg of DNP-HSA in 100 µl of 2% Evans Blue in saline. Mice were sacrificed 30 minutes after the

challenge by cervical dislocation and ear biopsies collected. Evans blue was extracted in 400 µl of formamide at 55°C for 24 hours and quantified by absorption at 595 nm.

6.10.3 Blood pressure and body temperature measurements

We used a radiotelemetry system (PA-C10, Data Sciences International) to monitor blood pressure in conscious, unrestrained mice as described previously [171].

For implantation of the pressure sensing catheter and the subcutaneous transmitter, mice were anesthetized with ketamine (i.p. 100 mg/kg) and xylazine (i.p. 10 mg/kg), and the neck was shaved and disinfected. Animals were placed on their backs on a heating plate, and the forelimbs were secured with tape. A piece of surgical thread was looped around the upper incisors and anchored to the table surface to allow easier access to the region around carotid artery. A ventral midline skin incision was made from the lower mandible posterior to the sternum. The left common carotid artery was isolated with blunt forceps. Care was taken not to disturb the vagal nerve running parallel to the artery. Two silk ligatures (6/0, Fine Science Tools, Heidelberg, Germany) were passed under the carotid artery and used for ligation and retraction. The artery was ligated just caudal to the bifucation of the interior and exterior carotid arteries (anterior suture). Another, posterior suture was placed loosely about 0.5 cm from the first ligation and used for temporary occlusion of the artery during catheter insertion. To slightly retract and lift the vessel, gentle tension was applied to both ligatures. A tiny incision was made in the carotid artery next to anterior suture, and after removing the protective cover from the catheter, it was inserted into the carotid artery. The occlusive posterior suture was released, and the catheter was advanced to its right position in the carotid artery, the pressure- sensing tip just inside the thoracic

aorta. The loose ends of both anterior and posterior sutures were tied securely around the catheter.

A subcutaneous pouch was formed through the same ventral neck incision for placement of transmitter in animal's right flank. A pair of blunt scissors was used to gently dissect the skin free from underlying tissue. The transmitter was slipped under the skin and down into the pocket along the flank. A small drop of glue (3M Vetbond, 3M Animal Care Products, St. Paul, Michigan, USA) was added on the catheter in the right neck region to secure the device. The incision in the neck was closed with surgical thread (5/0, Marlin Violet, Catgut GmbH, Markneukirchen, Germany). Mice were kept on a heating plate and monitored carefully until recovered from anaesthesia.

After a recovery period of at least 1 week, arterial pressure recordings were collected, stored and analyzed with Dataquest A.R.T. software 4.0. We collected data for basal blood pressure measurements with a 10-s scheduled sampling every 5 minutes and used the 24-h mean values for analysis. For analyzing the acute effects of agonists and anaphylactic shock, we collected data continuously in 5-s intervals for different periods as indicated in the figures. The body temperature was measured with a temperature control module (TKM-0902) (Föhr Medical Instruments GmbH, Seeheim, Germany).

6.10.4 Passive systemic anaphylaxis

In order to induce passive systemic anaphylaxis, mice were injected i.v. with 20 µg of anti-DNP-HSA IgE in 100 µl of sterile 0.9% NaCl under short CO_2 anaesthesia. After 24 hours these passively immunized mice were challenged by a further i.v. injection of 1 mg of DNP-HSA in 100µl of saline. Control mice were injected with

saline and challenged as described for immunized mice. For determining hematocrit, blood samples were collected 10 minutes after challenge. The blood was analyzed in the central laboratory of the University of Heidelberg. Blood pressure measurements were done using the telemetric system.

6.10.5 Active systemic anaphylaxis

For inducing active systemic anaphylaxis, I first immunized mice with i.v. injection of 1 mg BSA and an adjuvant (300 ng pertussis toxin). After 14 days we challenged the mice with another i.v. injection of 2 mg BSA. We monitored the body temperature and survival of the mice for 120 min after the challenge.

6.10.6 Intravital microscopy

For studying leukocyte rolling in the cremaster muscle, male mice were anesthetized with an i.p. injection of ketamine (125 mg/kg) and xylazine (12.5 mg/kg). The trachea and the carotid artery were cannulated to facilitate spontaneous respiration and for injection of anaesthetics, antibodies, and saline. During the preparation of cremaster muscle and following intravital microscopy, mice were kept warm by placing them on a 36°C thermoplate. The cremaster muscle was carefully prepared for intravital microscopy as described previously [172]. The scrotum was held up with forceps away from cremaster muscle and longitudinally cut open. The connective tissue surrounding the cremaster was carefully separated by blunt dissection after which the cremaster was picked up and cut with scissors while avoiding the larger vessels. The incised cremaster was pinned to a plastic tray with needles for visualization with microscope. During the preparation and intravital microscopy, the cremaster was superfused with 36°C bicarbonate-buffered saline. The surgical preparation of the cremaster muscle

caused trauma induced inflammation reaction and P-selectin-dependent leukocyte rolling in the venules of cremaster muscle.

An intravital microscope (Axioskop, Carl Zeiss Inc, Thornwood, New York, USA) with a saline immersion x40 objective with 0.75 numerical aperture was used to make microscopic observations. Venules with diameters between 20 µm and 40 µm were observed and recorded through a charge-coupled device (CCD) camera system (model VE-1000CD, Dage-MTI Inc., Michigan City, Indiana, USA) for 60 seconds each using a video recorder (S-VHS recorder, Panasonic Osaka, Japan). At the end of experiment, the mouse was injected i.v. with anti-murine P-selectin RB40.34 antibody (rat IgG1 30 µg/mouse) in order to ensure that observed leukocyte rolling was P-selectin dependent. After antibody injection three additional vessels were recorded for analysis. Blood samples (10 µl) were taken via the carotid artery catheter before and after administration of P-selectin antibody and stained with Giemsa stain for systemic leukocyte count.

6.10.6.1 Data Analysis

Microvessel diameters, lengths, and rolling leukocyte velocities were measured from video recordings using a digital image–processing system [173]. The rolling leukocyte flux fraction was determined as described previously [136] from video recordings by counting all rolling leukocytes passing a line perpendicular to the vessel axis and dividing this number by the total leukocyte flux through the vessel, which was estimated as $WBC \times v_b \times \pi \times (d/2)^2$, where WBC was the systemic leukocyte count, v_b was the mean blood flow velocity, and d the venular diameter. The rolling flux fraction represents the fraction of rolling leukocytes as a percentage of all leukocytes passing through the microvessel per unit time. Wall shear rate (γ_w) was estimated as $2.12(8\, v_b/d)$, where v_b was the mean blood flow velocity, d the

venular diameter, and 2.12 a median empirical correction factor obtained from velocity profiles measured in microvessels *in vivo*. Individual leukocyte rolling velocities were measured from video recordings by randomly choosing 5 to 10 leukocytes per venule and measuring the time necessary to travel a fixed distance. Centreline blood flow velocity was measured with a dual photodiode and a digital online cross-correlation program (CircuSoft Instrumentation LLC, Hockessin, Delaware, USA). Adherent leukocytes in the venules were counted.

7 RESULTS

7.1 Purity of the primary endothelial cell culture and loss of G_q/G_{11} and G_{12}/G_{13} in endothelial cells

In order to study roles of G_q/G_{11}- and G_{12}/G_{13}-mediated signalling in endothelial cells *in vitro*, we generated primary mouse pulmonary endothelial cells lacking the α-subunits of G_q/G_{11} and G_{12}/G_{13}. We used mice with floxed alleles for the genes encoding $G\alpha_q$ (*Gnaq*) and $G\alpha_{13}$ (*Gna13*) which facilitate the conditional inactivation of these genes in $G\alpha_{11}$- or $G\alpha_{12}$-deficient backgrounds as previously described [18, 166]. I isolated mouse primary pulmonary endothelial cells as described in Materials and Methods. Endothelial cells are known to be able to take up low density lipoprotein (LDL) [174], therefore the purity of the primary endothelial cell cultures was analyzed by incubating endothelial cells with fluorescently labelled LDL and DAPI. In addition endothelial cells were stained with VE-cadherin (CD144) antibody that is known to be expressed exclusively in endothelial cells [39].

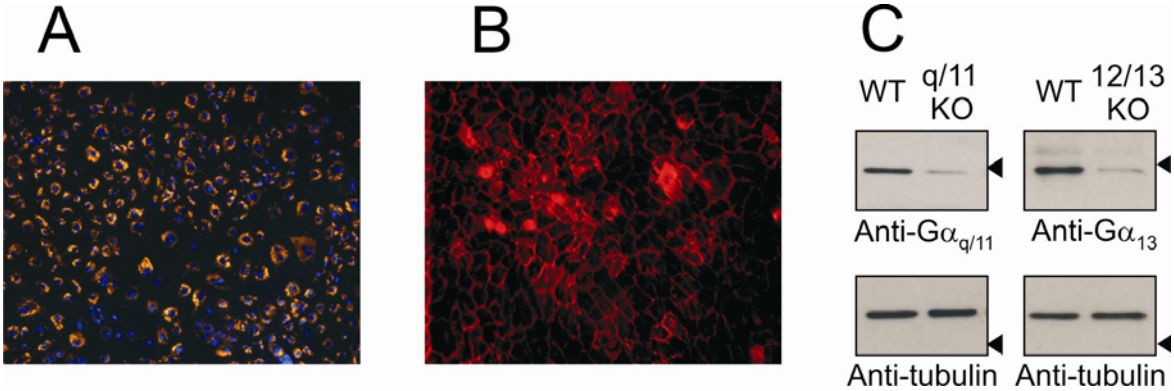

Figure 6. Analysis of the purity of the primary endothelial cell cultures and protein expression in endothelial cells. Shown is an example of wild-type endothelial cells incubated with fluorescently labelled LDL (red) and DAPI (blue) (A), or with VE-cadherin antibody (red) (B). (C) Western blot analysis of wild-type (WT), *Gnaq*$^{flox/flox}$;*Gna11*$^{-/-}$ (q/11 KO) and *Gna12*$^{-/-}$;*Gna13*$^{flox/flox}$ (12/13 KO) endothelial cells infected with Cre expressing adenovirus. Antibodies were directed against $G\alpha_{q/11}$, $G\alpha_{13}$, and α-tubulin. Arrow heads indicate the position of the 43 kDa marker protein.

The purity of the endothelial cell cultures was generally about 90-95% (Figure 6 A and B). In order to induce $G\alpha_q/G\alpha_{11}$ or $G\alpha_{12}/G\alpha_{13}$ double deficiency, I infected pulmonary microvascular endothelial cells from wild-type, *Gnaq*$^{flox/flox}$;*Gna11*$^{-/-}$ and *Gna12*$^{-/-}$;*Gna13*$^{flox/flox}$ mice with an adenovirus transducing the Cre recombinase. I then analyzed protein expression in pulmonary endothelial cell lysates by Western blot. As shown in Figure 6 C, expression of Cre recombinase in *Gnaq*$^{flox/flox}$;*Gna11*$^{-/-}$ or *Gna12*$^{-/-}$;*Gna13*$^{flox/flox}$ endothelial cells resulted in $G\alpha_q/G\alpha_{11}$ and $G\alpha_{13}$ deficiency, respectively.

7.2 G_q/G_{11} primarily mediate endothelial effects of inflammatory mediators acting via GPCRs

To analyze G_q/G_{11}- and G_{12}/G_{13}-mediated signalling in endothelial cells in response to various vasoactive mediators, we used $G\alpha_q/G\alpha_{11}$- or $G\alpha_{12}/G\alpha_{13}$-deficient pulmonary endothelial cells generated as described in Materials and Methods.

The phosphorylation state of MLC is a critical determinant of endothelial cell contractility. I thus stimulated wild-type, $G\alpha_q/G\alpha_{11}$- and $G\alpha_{12}/G\alpha_{13}$-deficient endothelial cells with thrombin (1 U/ml) for indicated times and performed Western blots to detect the MLC phosphorylation in endothelial cells. As shown in Figure 7, thrombin induced a rapid increase in MLC phosphorylation in wild-type cells. The effect of thrombin was maximal after about 3 minutes. In contrast thrombin did not induce MLC phosphorylation in endothelial cells lacking $G\alpha_q/G\alpha_{11}$. $G\alpha_{12}/G\alpha_{13}$ deficiency did not completely block thrombin-induced MLC phosphorylation but led to a reduced and more transient response to thrombin.

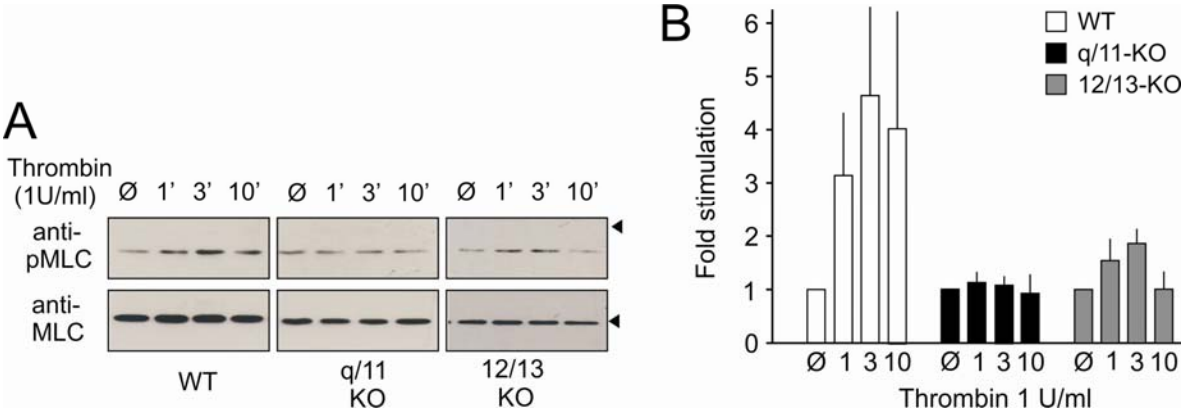

Figure 7. Western blot analysis of thrombin stimulated wild-type, $G\alpha_q/G\alpha_{11}$- and $G\alpha_{12}/G\alpha_{13}$-deficient endothelial cells. Endothelial cells from wild-type (WT), $G\alpha_q/G\alpha_{11}$- (q/11 KO) and $G\alpha_{12}/G\alpha_{13}$-deficient (12/13 KO) mice were stimulated with 1U/ml thrombin for indicated times. (A) Arrow heads indicate the position of the 25 kDa (pMLC) and the 17 kDa (MLC) marker proteins. Data shown are from at least 3 independently performed experiments. (B) Quatification of MLC phosphorylation from 3 independent experiments.

We also analyzed G_q/G_{11} and G_{12}/G_{13}-mediated signalling in endothelial cells upstream of MLC phosphorylation. MLC phosphorylation is dually regulated by two signalling pathways: IP_3/Ca^{2+} and MLC kinase or RhoA and MLC phosphatase [9]. Therefore I treated wild-type, $G\alpha_q/G\alpha_{11}$- and $G\alpha_{12}/G\alpha_{13}$-deficient endothelial cells with or without 1U/ml thrombin, lysed the cells and afterwards measured IP_3 formation and RhoA activation as described in Materials and Methods. Lack of $G\alpha_q/G\alpha_{11}$ in endothelial cells blocked thrombin-induced IP_3 production, while $G\alpha_{12}/G\alpha_{13}$-deficient endothelial cells responded comparable to wild-type cells (Figure 8 A). Interestingly, thrombin-induced RhoA activation was abrogated in endothelial cells lacking $G\alpha_{12}/G\alpha_{13}$, but the $G\alpha_{12}/G\alpha_{13}$-deficient endothelial cells were still able to phosphorylate MLC (Figure 8 B and Figure 7). The abrogation of thrombin-induced myosin light chain phosphorylation in cells lacking $G\alpha_q/G\alpha_{11}$ was not accompanied by any defect in thrombin-induced RhoA activation (Figure 7 and Figure 8 B).

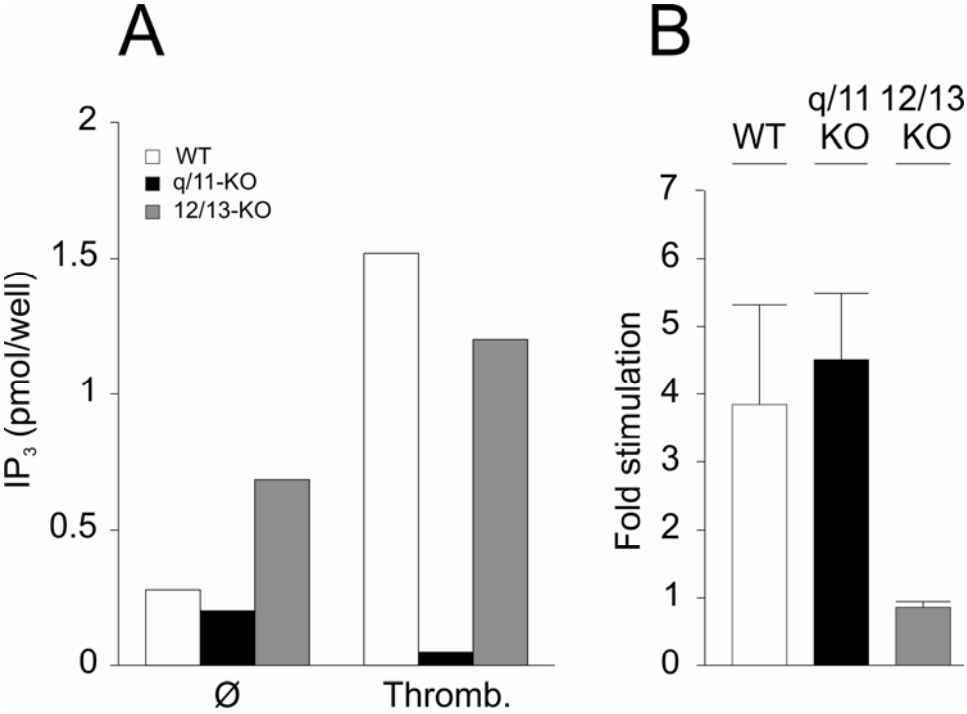

Figure 8. IP3 formation and RhoA activation in endothelial cells. (A) Shown is IP3 formation in thrombin (Thromb.) stimulated wild-type, $G\alpha_q/G\alpha_{11}$- and $G\alpha_{12}/G\alpha_{13}$-deficient endothelial cells. Shown is an example of a typical experiment. (B) RhoA activation expressed as fold stimulation in thrombin stimulated wild-type (WT), $G\alpha_q/G\alpha_{11}$- (q/11 KO) and $G\alpha_{12}/G\alpha_{13}$-deficient (12/13 KO) endothelial cells. Data shown are from 3 independent experiments (mean values ± SEM).

NO formation plays a critical role in anaphylactic shock. However, the source of NO in anaphylaxis has been unclear [175]. We thus analyzed the role of G_q/G_{11}- and G_{12}/G_{13}-mediated signalling in endothelial NO production in response to stimuli known to act via GPCRs. We determined NO-dependent activation of guanylyl cyclase using a transfer bioassay. In this assay RFL6 reporter fibroblasts were incubated with wild-type, $G\alpha_q/G\alpha_{11}$-, or $G\alpha_{12}/G\alpha_{13}$-deficient lung endothelial cells. Endothelial cells were treated with or without thrombin, PAF or ionomycin, and cGMP levels were measured with radioimmunoassay (Figure 9). Thrombin and PAF induced a significant increase in cGMP levels of RFL6 fibroblasts co-cultured with wild-type and $G\alpha_{12}/G\alpha_{13}$-deficient endothelial cells. In contrast the effects of thrombin and PAF in co-cultures containing $G\alpha_q/G\alpha_{11}$-deficient endothelial cells

were strongly reduced. None of the stimuli induced cGMP production when added to RFL6 fibroblasts or endothelial cells alone (data not shown). Positive control ionomycin induced similar effects in wild-type, $G\alpha_q/G\alpha_{11}$- and $G\alpha_{12}/G\alpha_{13}$-deficient endothelial cells. Our results indicate that G_q/G_{11} but not G_{12}/G_{13} are critically involved in thrombin- and PAF-induced endothelial NO formation measured indirectly by production of guanylyl cyclase in RFL6 fibroblasts.

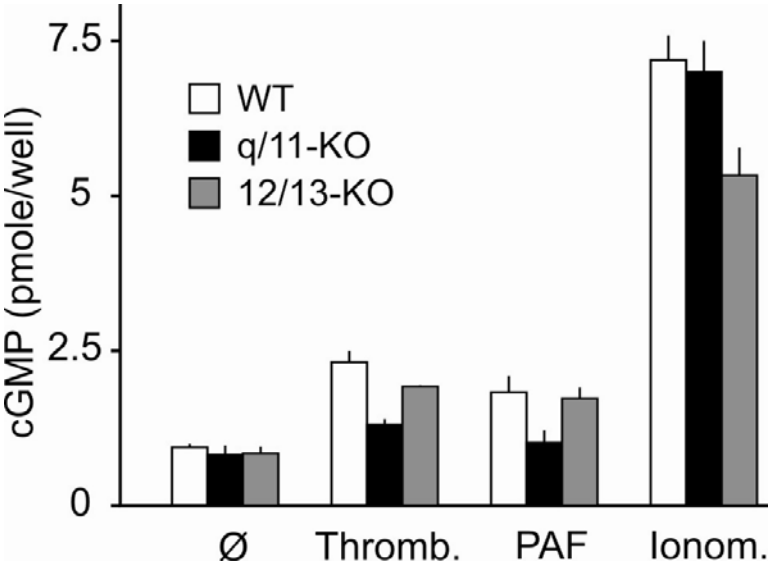

Figure 9. The role of G_q/G_{11} and G_{12}/G_{13} in the regulation of NO production. Pulmonary endothelial cells from wild-type, $G\alpha_q/G\alpha_{11}$- and $G\alpha_{12}/G\alpha_{13}$-deficient mice were stimulated with or without 1 U/ml thrombin (Thromb.), 100 nM PAF, or 100 nM ionomycin (Ionom.). NO formation was assessed by determining cGMP production in reporter RFL6 fibroblasts by radioimmunoassay. Shown is an example of 3 independent experiments with reproducible results (mean values ± SD).

7.3 Generation and genotyping of mice with endothelial cell specific $G\alpha_q/G\alpha_{11}$ and $G\alpha_{12}/G\alpha_{13}$ deficiency

For *in vivo* experiments, we generated endothelial cell specific $G\alpha_q/G\alpha_{11}$ and $G\alpha_{12}/G\alpha_{13}$ double knock-out mice by using a mouse line which expresses a fusion protein of the Cre recombinase with the modified estrogen receptor binding domain (*Cre*ER^{T2}) [176] under the control of the *tie2* promoter. We crossed *tie2-Cre*ER^{T2} mice with mice carrying floxed alleles for the genes encoding $G\alpha_q$ (*Gnaq*)

and $G\alpha_{13}$ (*Gna13*). This facilitated the conditional inactivation of these genes in $G\alpha_{11}$- or $G\alpha_{12}$-deficient backgrounds as previously described [18, 166]. In order to determine the genotypes of the offspring from these matings, we performed PCRs as described in the Materials and Methods. In Figure 10 the typical results of genotyping PCRs are shown.

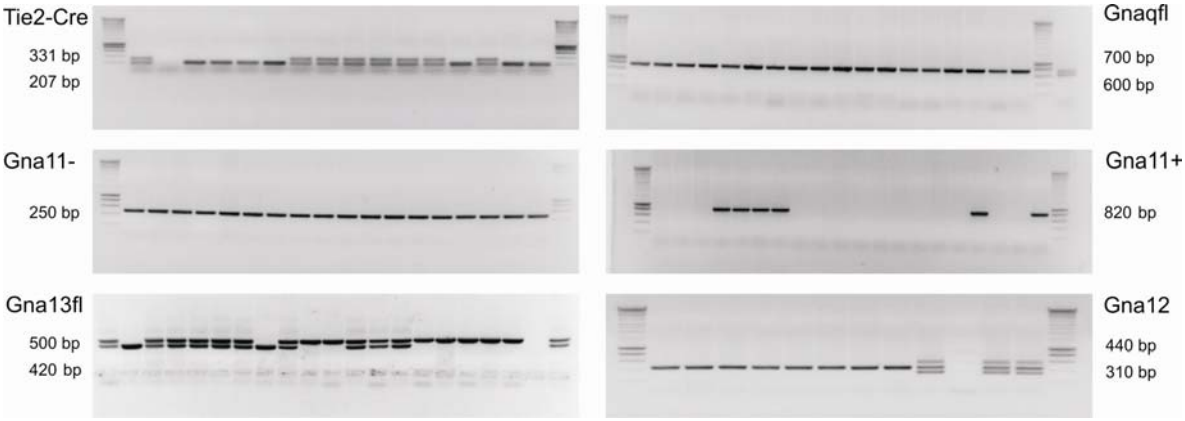

Figure 10. Generation of mice with endothelial cell-specific $G\alpha_q/G\alpha_{11}$ and $G\alpha_{12}/G\alpha_{13}$ deficiency. Shown are the typical genotyping results of endothelial cell-specific $G\alpha_q/G\alpha_{11}$ and $G\alpha_{12}/G\alpha_{13}$ - deficient mice. (A) Tie2-Cre: WT allele 331 bp, mutant allele 207 bp, (B) $Gnaq^{fl}$: mutant allele 700 bp, WT allele 600 bp, (C) $Gna11^{+}$: WT allele 820 bp, (D) $Gna11^{-}$: null allele 250 bp, (E) $Gna13^{fl}$: mutant allele 500 bp, WT allele 420 bp , and (F) Gna12: WT allele 440 bp, null allele 310 bp.

In order to induce Cre-mediated recombination I treated the mice with tamoxifen (1 mg/day) for 5 consecutive days and sacrificed the mice 14 days after the beginning of induction. I then analyzed β-galactosidase activity on cryosections of different organs. I observed Cre-mediated recombination exclusively in endothelial cells of various organs as shown in Figure 11 A. Cre-mediated recombination could not be observed in brain or aorta. I also analyzed β-galactosidase activity in immune cells from the blood. The immune cells did not show Cre recombination 9 days after induction with tamoxifen (Figure 11 B).

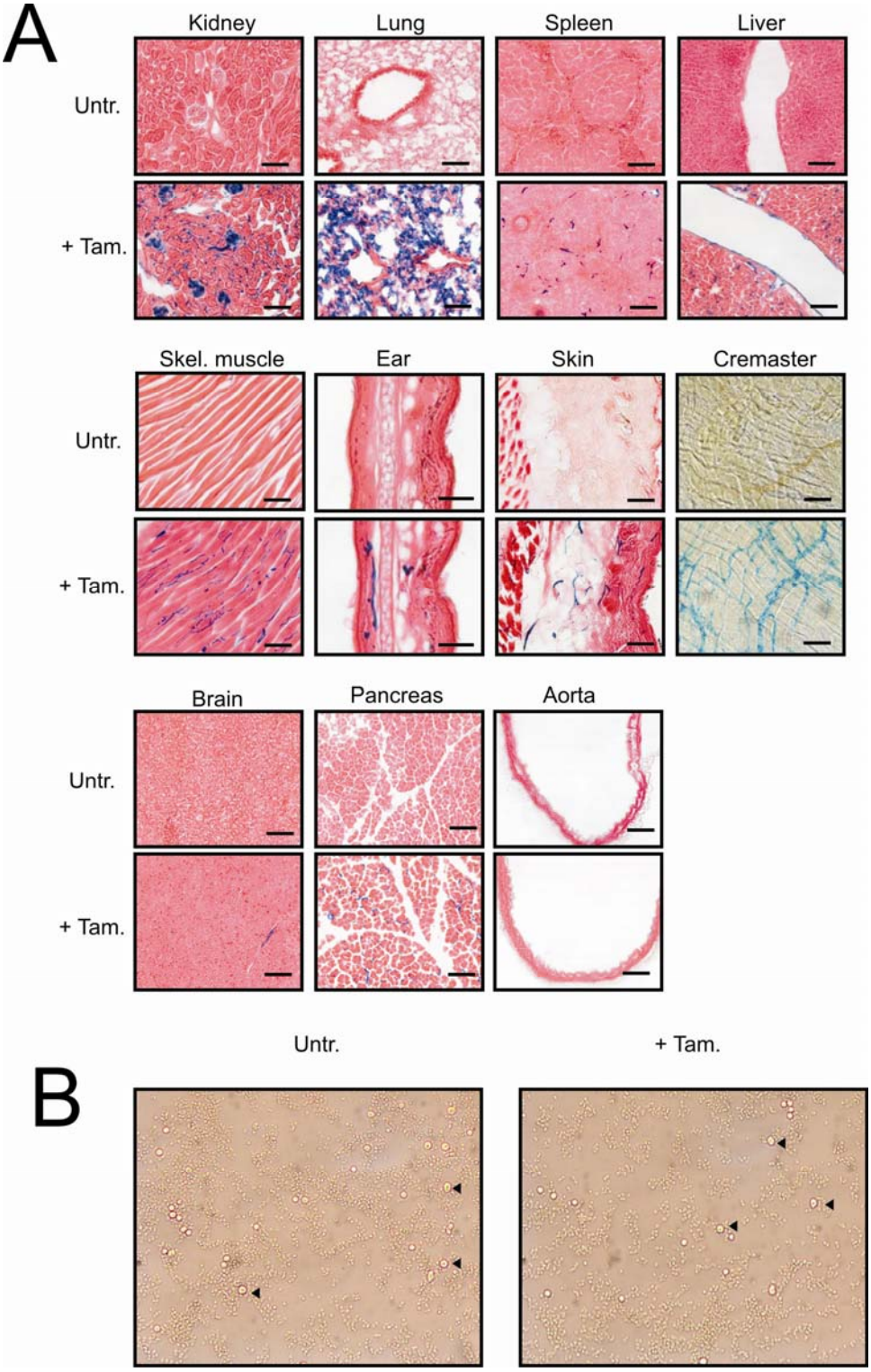

Figure 11. Analysis of β-galactosidase activity. Gt(ROSA26)SorCre reporter mice carrying the tie2-CreER^{T2} transgene were treated with tamoxifen (+Tam.) or vehicle (untr.) and sacrificed. (A)The indicated organs were sectioned and stained for β-galactosidase activity (blue). (B) Bloodsmear,stained for β-galactosidase activity. Arrowheads indicate leukocytes.

I then analyzed the expression of $G\alpha_q/G\alpha_{11}$ and $G\alpha_{13}$ in endothelial cells isolated from tamoxifen-treated wild-type, *tie2-Cre*ER^{T2};*Gnaq*$^{flox/flox}$;*Gna11*$^{-/-}$ (EC-$G\alpha_q/G\alpha_{11}$-KO) and *tie2-Cre*ER^{T2};*Gna12*$^{-/-}$;*Gna13*$^{flox/flox}$ (EC-$G\alpha_{12}/G\alpha_{13}$-KO) mice. I lysed pulmonary endothelial cells prepared from the respective mouse lines and determined the protein expression by Western blotting. As shown in Figure 12, tamoxifen treatment of EC-$G\alpha_q/G\alpha_{11}$-KO and EC-$G\alpha_{12}/G\alpha_{13}$-KO mice induced $G\alpha_q/G\alpha_{11}$ and $G\alpha_{13}$ deficiency, respectively.

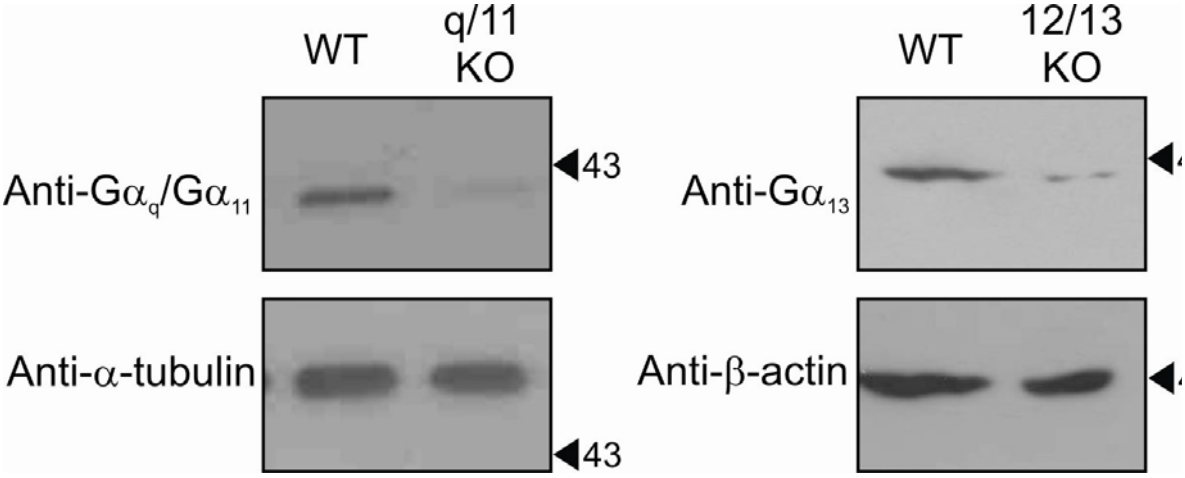

Figure 12. Analysis of protein expression in the endothelial cells isolated from tamoxifen treated animals. Lysates of pulmonary endothelial cells isolated from wild-type (WT), $G\alpha_q/G\alpha_{11}$ (q/11 KO) and $G\alpha_{12}/G\alpha_{13}$-deficient (12/13 KO) mice. Antibodies used were directed against $G\alpha_{q/11}$, $G\alpha_{13}$, α-tubulin, and β-actin. Arrows indicate the position of 43 kDa marker protein.

7.4 $G\alpha_q/G\alpha_{11}$ deficiency blocks local extravasation in response to various stimuli

Next I analyzed the effects of several vascular permeability increasing substances on the local extravasation in wild-type, EC-$G\alpha_q/G\alpha_{11}$-KO and EC-$G\alpha_{12}/G\alpha_{13}$-KO mice. I injected anesthetised mice i.v. with Evans blue dye (0.04µg/g). Subsequently, mice were injected intradermally with lysophosphatidic acid (LPA), the protease-activated receptor-1 activating peptide SFLLRN-NH_2, histamine, or PAF. After 10 min mice were sacrificed and skin pieces containing the injection sites were collected. Evans blue dye was extracted with formamide as described in Materials and Methods. Each agonist induced a dose-dependent increase in the leakage of Evans blue dye in the wild-type and EC-$G\alpha_{12}/G\alpha_{13}$-KO mice (Figure 13 A-D). Basal vascular permeability and the stimulus-induced vascular permeability were reduced in mice with endothelial-specific $G\alpha_q/G\alpha_{11}$ deficiency. The small remaining response to the PAR1-activating peptide observed in EC-$G\alpha_q/G\alpha_{11}$-KO mice was not further reduced in mice lacking both $G\alpha_q/G\alpha_{11}$ and $G\alpha_{12}/G\alpha_{13}$ in endothelial cells (Figure 13 D).

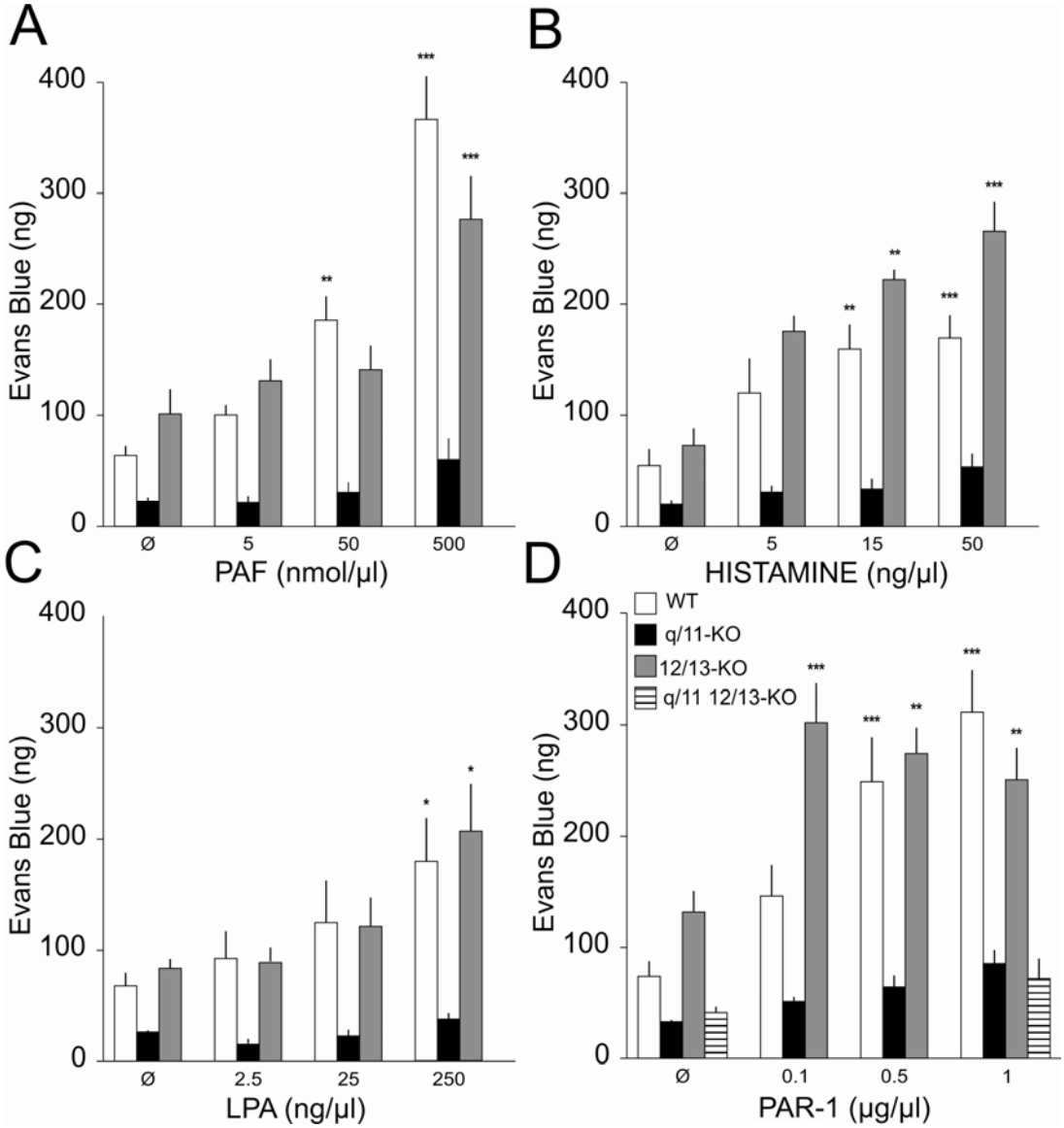

Figure 13. Endothelial permeability in endothelial cell-specific G$\alpha_{q/11}$- and G$\alpha_{12/13}$-deficient mice. Mice were intradermally stimulated with PAF (A), histamine (B), LPA (C), and PAR-1 (D). Shown are the amounts of Evans blue extracted from skin explants. Values are means ± s.e.m.; * p<0.05, ** p<0.01, *** p<0.001 (compared to basal).

We then tested the regulation of the endothelial barrier permeability in a more physiological model of local anaphylaxis. In order to induce anaphylactic reaction, I first sensitized mice by a local intradermal injection of anti-DNP IgE antibodies. After 24 hours, I subsequently challenged the mice with i.v. injection of DNP-HSA. DNP-HSA challenge resulted in increased permeability determined as increased

extravasation of Evans blue dye in the ears of wild-type mice. EC-Gα_{12}/Gα_{13}-KO mice showed normal permeability increase that was comparable to the response of wild-type mice. In contrast the mice with endothelium-specific Gα_q/Gα_{11} deficiency showed strongly reduced vascular permeability (Figure 14). Our results suggest that local regulation of vascular permeability requires G_q/G_{11}-mediated signalling in endothelial cells but not G_{12}/G_{13}.

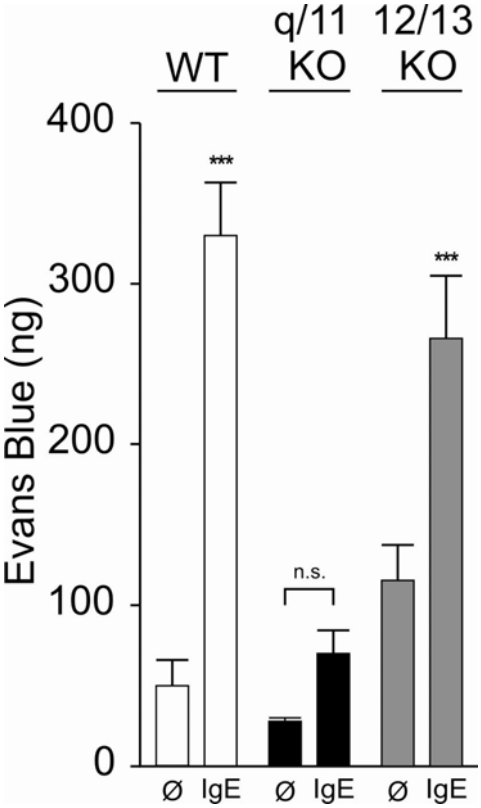

Figure 14. Endothelial permeability in the model of local anaphylaxis. Mice were sensitized by intracutaneous injection of anti-DNP IgE antibodies. DNP-HSA challenge was administered 24 h by i.v. injection. Evans blue contents in the ears of wild-type (WT), Gα_q/Gα_{11} (q/11 KO) and Gα_{12}/Gα_{13}-deficient (12/13 KO) mice were quantified by absorption at 595 nm. Values are means ± s.e.m.; *** p<0.001 (compared to basal).

7.5 Basal blood pressure is unchanged in $G\alpha_q$/$G\alpha_{11}$and $G\alpha_{12}$/$G\alpha_{13}$-KO mice

In order to study the roles of $G\alpha_{q/11}$ and $G\alpha_{12/13}$ on basal functions of endothelium, I performed blood pressure measurements using telemetric system as described in Materials and Methods. After implantation of the pressure sensing catheter and transmitter, mice were allowed to recover for a week. Thereafter basal blood pressure was recorded before, during, and after tamoxifen treatment. Endothelial $G\alpha_{q/11}$- and $G\alpha_{12/13}$ -deficiency did not alter basal blood pressure of the knock-out mice. This indicated that $G\alpha_{q/11}$ and $G\alpha_{12/13}$ did not affect the regulation of blood pressure under physiological conditions (Figure 15).

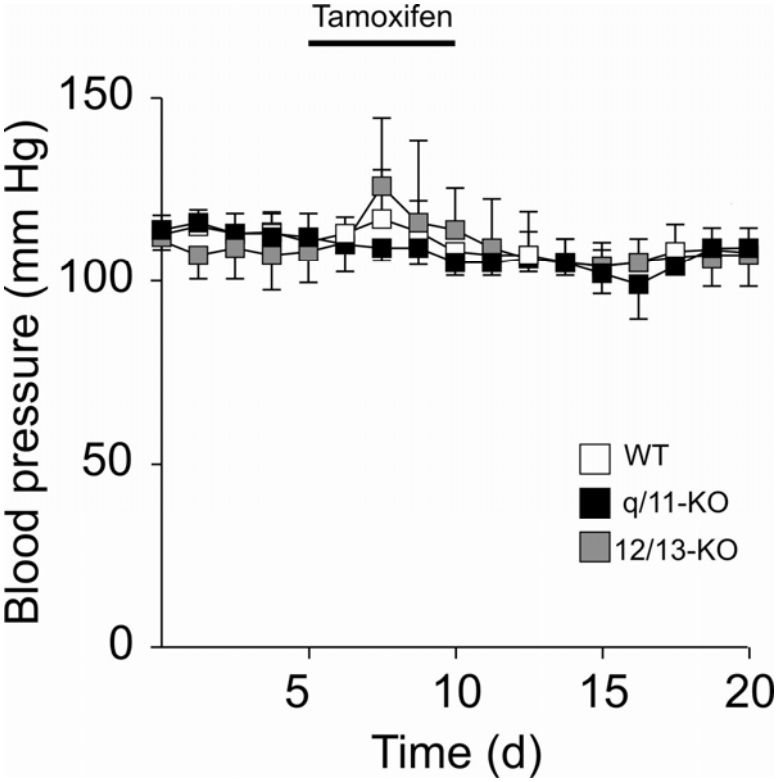

Figure 15. Recordings of basal blood pressure in wild-type and endothelial cell-specific $G\alpha_{q/11}$- and $G\alpha_{12/13}$-deficient mice. Shown are the mean values of 3 mice per genotype ± S.D..

7.6 Systemic effects of histamine and PAF, but not of LPS, are blocked in EC-$G\alpha_q/G\alpha_{11}$-KO mice

To study the blood pressure effects of histamine, one of the mediators of anaphylaxis, I injected wild-type, EC-$G\alpha_q/G\alpha_{11}$-KO and EC-$G\alpha_{12}/G\alpha_{13}$-KO mice i.v. with 10mg/kg histamine and recorded blood pressure of the mice by a radiotelemetry system. Intravenous injection of histamine induced a rapid and transient drop in the systolic blood pressure to levels of about 50 mm Hg in wild-type mice (Figure 16). Normal values were restored approximately 90 min after the application of histamine. In EC-$G\alpha_q/G\alpha_{11}$-KO mice, the same dose of histamine decreased blood pressure for only about 20 min with maximal hypotensive values of about 90 mm Hg. The response of EC-$G\alpha_{12}/G\alpha_{13}$-KO mice to i.v. histamine injection was comparable to wild-type mice (Figure 16).

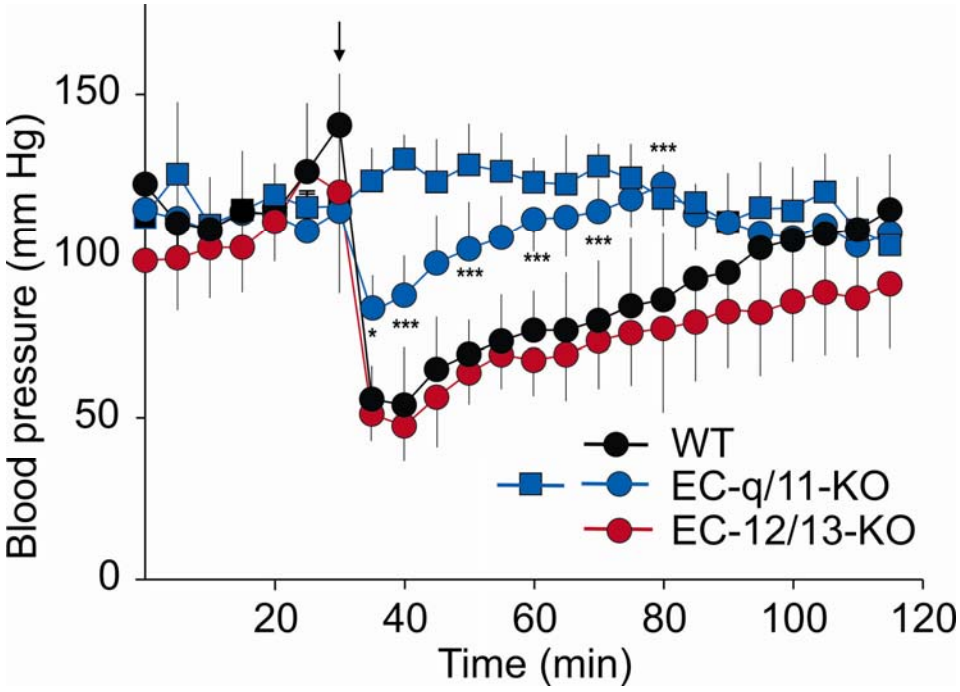

Figure 16. Effects of histamine on blood pressure. Systolic blood pressure was recorded telemetrically in mice before and after injection of carrier solution (squares) or 10 mg/kg histamine (circles). Shown are mean values of 5-7 mice per genotype ± S.D.; * p<0.05, ** p<0.01, *** p<0.001 (compared to WT). The arrow indicates the time point of histamine administration.

Since the hypotensive response of EC-Gα_q/Gα_{11}-KO mice to histamine was strongly reduced, we wanted to ensure that EC-Gα_q/Gα_{11}-KO mice did not suffer from a general defect in the regulation of the vascular tone. Therefore we decided to analyze the effects of the NO-donator sodium nitroprusside (SNP) and the NO-synthase inhibitor N^{ω}-nitro-L-arginine methyl ester (L-NAME) on blood pressure of wild-type, EC-Gα_q/Gα_{11}-KO and EC-Gα_{12}/Gα_{13}-KO mice. I recorded blood pressure of the mice before and after injection of SNP and L-NAME. Wild-type, EC-Gα_q/Gα_{11}-KO and EC-Gα_{12}/Gα_{13}-KO showed indistinguishable responses to SNP and L-NAME, indicating that there was no general defect in the regulation of blood pressure in EC-Gα_q/Gα_{11}-KO mice (Figure 17).

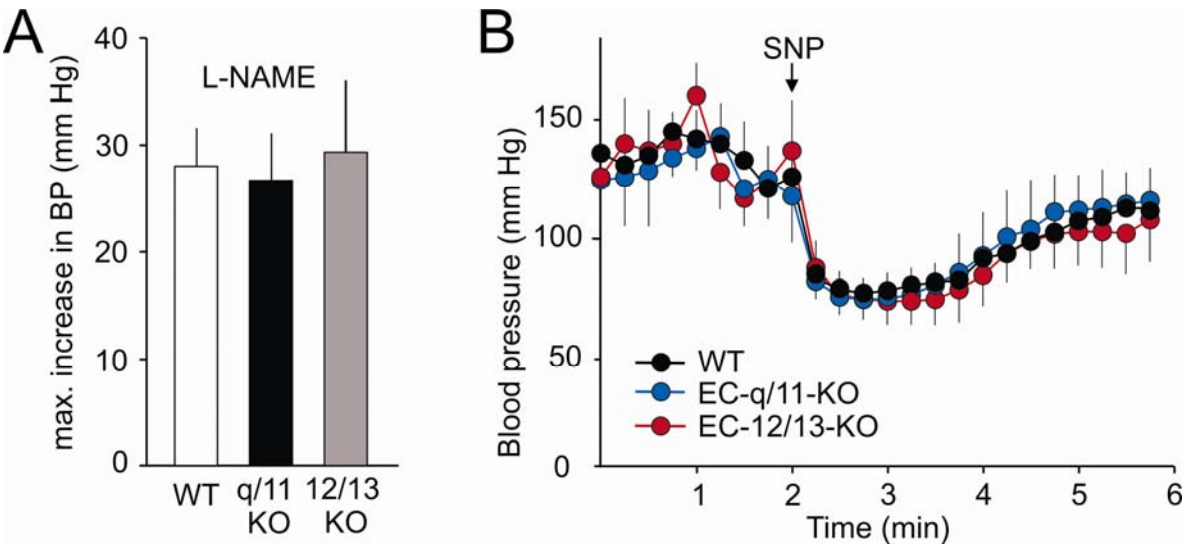

Figure 17. Effects of L-NAME and sodium nitroprusside (SNP) on blood pressure. Systemic blood pressure was recorded telemetrically in mice before and after i.v. administration of L-NAME (A) or SNP (B). (A) Shown is maximal change in blood pressure (mm Hg) after i.v. injection of 50 mg/kg L-NAME in anesthetised mice. Values are means ± S.D from 4-6 measurements per genotype. (B) Shown is the systemic blood pressure before and after i.v. injection of 1 mg/kg SNP. Values are means from 5-8 measurements per genotype ± S.D.

We then set to test another mediator involved in anaphylaxis, platelet activating factor (PAF), which is thought to be a critical mediator of anaphylactic shock [157, 177, 178]. I analyzed the effect of endothelium-specific Gα_q/Gα_{11} and Gα_{12}/Gα_{13}

deficiency on the systemic response to PAF. I injected wild-type, EC-Gα_q/Gα_{11}-KO and EC-Gα_{12}/Gα_{13}-KO mice i.v. with 1.9 µg/kg PAF and measured the body temperature and monitored the survival of the mice. Intravenous injection of PAF induced severe hypothermia and resulted in the death of wild-type and EC-Gα_{12}/Gα_{13}-KO mice within 20 min (Figure 18 A). However, mice with endothelial Gα_q/Gα_{11} deficiency were protected from PAF-induced shock, and all tested animals survived the injection of PAF with only a transient drop in body temperature (Figure 18 A and B). I also injected mice lacking only Gα_{11} with PAF, in order to test if Gα_{11} deficiency alone had a protective effect on anaphylactic shock. Gα_{11}-deficient mice showed an intermediate phenotype with more severe hypothermia than EC-Gα_q/Gα_{11}-KO mice and a survival rate of only 25% (2 of 8 tested animals, Figure 18 B).

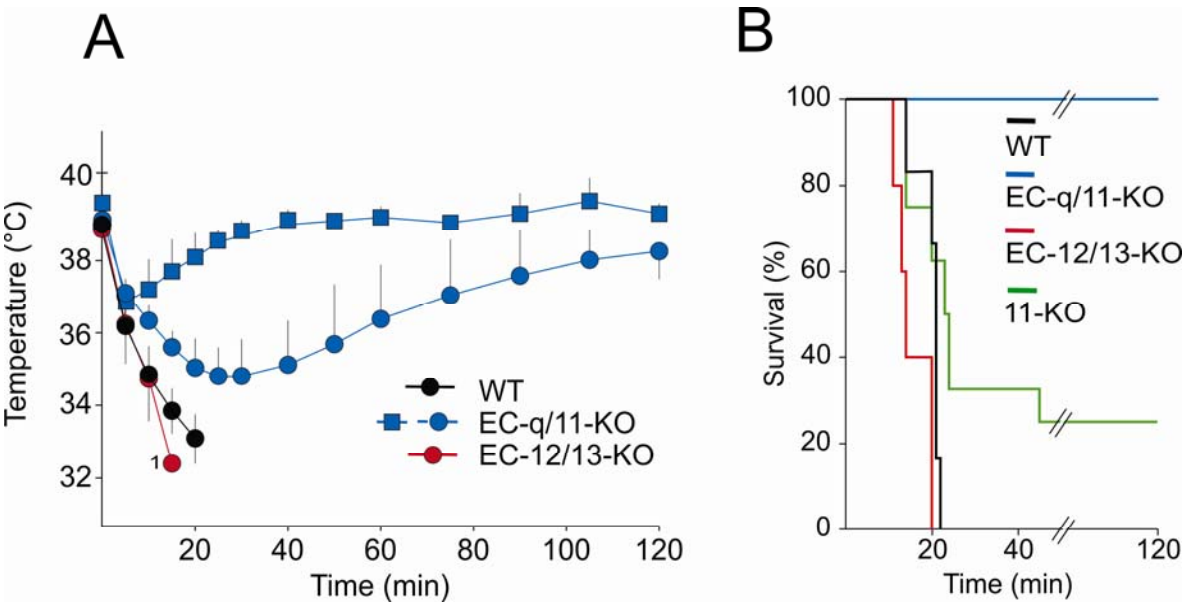

Figure 18. Role of endothelial G_q/G_{11} and G_{12}/G_{13} in the systemic effects of PAF. 5-6 mice per genotype were injected i.v. with 1.9 µg/g PAF and the body temperature (A) and survival (B) of the mice were monitored for 120 min. Numbers below the time points of the temperature blot show the number of animals still alive at the indicated time points. Show are mean values ± S.D. (A).

7.7 Anaphylactic shock depends on endothelial G_q/G_{11}

To further evaluate the role of endothelial $G\alpha_q/G\alpha_{11}$ and $G\alpha_{12}/G\alpha_{13}$ deficiency under pathophysiologically more relevant conditions, we set up models for passive and active systemic anaphylaxis. We first tested the role of endothelial G_q/G_{11} and G_{12}/G_{13} in passive systemic IgE-dependent anaphylaxis. I immunized wild-type, EC-$G\alpha_q/G\alpha_{11}$-KO and EC-$G\alpha_{12}/G\alpha_{13}$-KO mice by i.v. injection of 20 µg anti-DNP IgE. 24 hours later I challenged the passively immunized mice with i.v. injection of 1 mg DNP-HSA. After DNP-HSA challenge, the systolic blood pressure of wild-type and EC-$G\alpha_{12}/G\alpha_{13}$-KO mice decreased rapidly. Within few minutes their systolic blood pressure dropped to values of about 35 mm Hg. After a while, the blood pressure started to slowly increase, but mice remained hypotensive for more than 90 min (Figure 19 A). Mice with endothelial $G\alpha_q/G\alpha_{11}$ deficiency were immunized and challenged in the same manner, but they showed only a minor and short lasting reduction in blood pressure (Figure 19 A).

Increase in hematocrit is one of the main symptoms of anaphylactic shock and it indicates severe extravasation of plasma. I collected blood samples from sensitized mice before and after DNP-HSA challenge for determination of hematocrit. As shown in , both wild-type and EC-$G\alpha_{12}/G\alpha_{13}$-KO mice showed a strong increase in their hematocrit after application of the allergen. The hematocrit of similarly treated EC-$G\alpha_q/G\alpha_{11}$-KO mice remained unchanged after allergen administration (Figure 19 B).

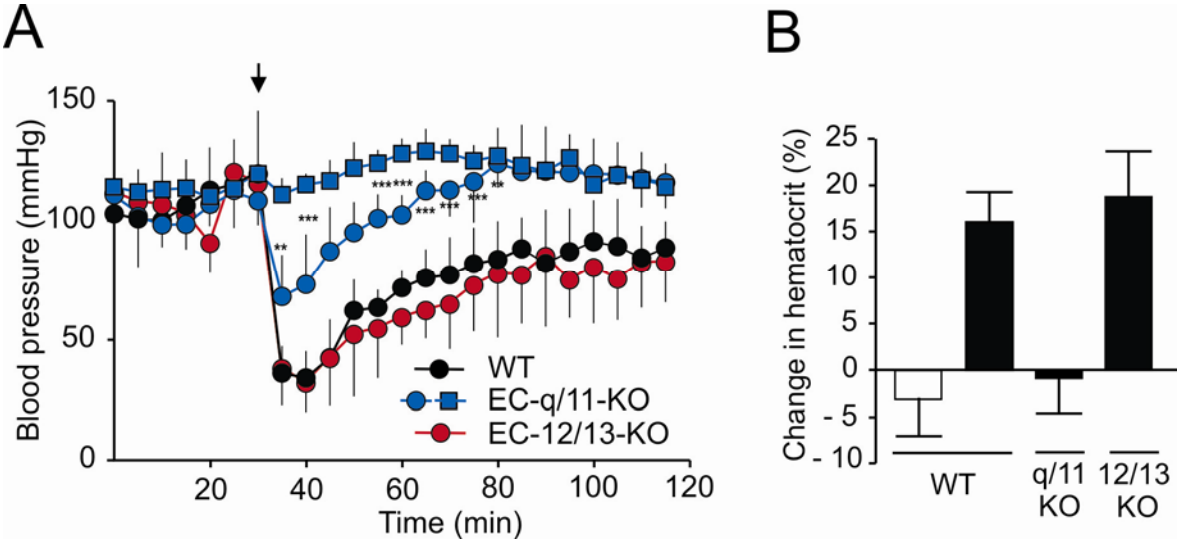

Figure 19. Analysis of systemic blood pressure and hematocrit in a model of passive systemic anaphylaxis. Wild-type, $G\alpha_{q/11}$- and $G\alpha_{12/13}$-deficient mice were sensitized with anti-DNP antibodies and challenged with i.v. injection of DNP-HSA (circles, black bars, respectively) or buffer (squares, white bars, respectively). (A) Systemic blood pressure of mice was recorded for indicated time before and after DNP-HSA challenge. Arrow indicates the time point of DNP-HSA administration. Data shown are mean values ± S.D from 6 WT, 5 q/11 KO, 4 12/13 KO, and 3 q/11 KO (buffer) mice. (B) Blood samples from wild-type, $G\alpha_{q/11}$- and $G\alpha_{12/13}$-deficient mice were collected before and after DNP-HSA challenge for determination of hematocrit. Data are expressed as mean values ± S.D from 6 WT, 5 q/11 KO, 6 12/13 KO, and 3 WT (buffer) mice.

In model of active systemic anaphylaxis, we sensitized mice with i.p. injection of 1 mg BSA together with adjuvant pertussis toxin (300 ng). Two weeks later, mice were challenged with an i.v. injection of the same allergen, and their temperature and survival were monitored. Few minutes after BSA challenge, all mice developed severe hypothermia (Figure 20 A). Wild-type and EC-$G\alpha_{12}$/$G\alpha_{13}$-KO mice died within 20 min after the challenge (Figure 20 B). However as shown in Figure A and B, EC-$G\alpha_{q}$/$G\alpha_{11}$-KO recovered from hypothermia after about 1 hour, and all of the tested animals (n=5) survived the challenge with allergen. Mice lacking only $G\alpha_{11}$ showed an intermediate phenotype and had a survival rate of 20% (2 of 10 animals).

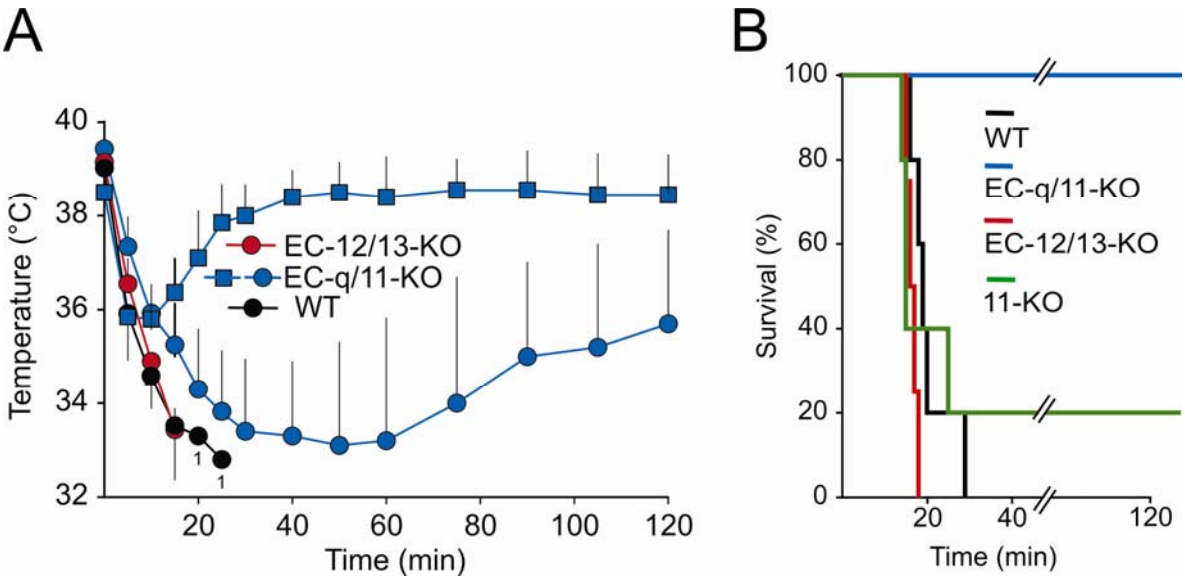

Figure 20. Analysis of body temperature and survival in a model of active systemic anaphylaxis. Wild-type, $G\alpha_{q/11}$- and $G\alpha_{12/13}$-deficient mice were sensitized with 1 mg BSA and adjuvant pertussis toxin (300 ng) and challenged 2 weeks later with i.v. injection of BSA. (A) The body temperature of the animals was measured before and after challenge at indicated time points. Data shown are mean values ± S.D from 5 WT, 5 q/11 KO, 4 12/13 KO, and 3 q/11 KO (buffer) mice. (B) The survival of the animals was monitored for the indicated time after the BSA challenge. Animal numbers were as in (A).

Because $G\alpha_q/G\alpha_{11}$ and $G\alpha_{12}/G\alpha_{13}$ deficiency was protective in PAF shock and in models of passive and active anaphylaxis, we also wanted to test whether $G\alpha_q/G\alpha_{11}$ and $G\alpha_{12}/G\alpha_{13}$ deficiency played a role in septic shock. NO has been suggested to play an important role during septic shock and affect the occurrence of death [163, 179]. We thus injected the mice intraperitoneally with the endotoxin lipopolysaccharide (LPS) and monitored blood pressure telemetrically for 25 hours. LPS injection induced a severe hypotension and eventual lethality in both wild-type and in EC-$G\alpha_q/G\alpha_{11}$-KO mice (Figure 21 and data not shown). Thus, endothelial $G\alpha_q/G\alpha_{11}$ deficiency did not play a role in endotoxic shock.

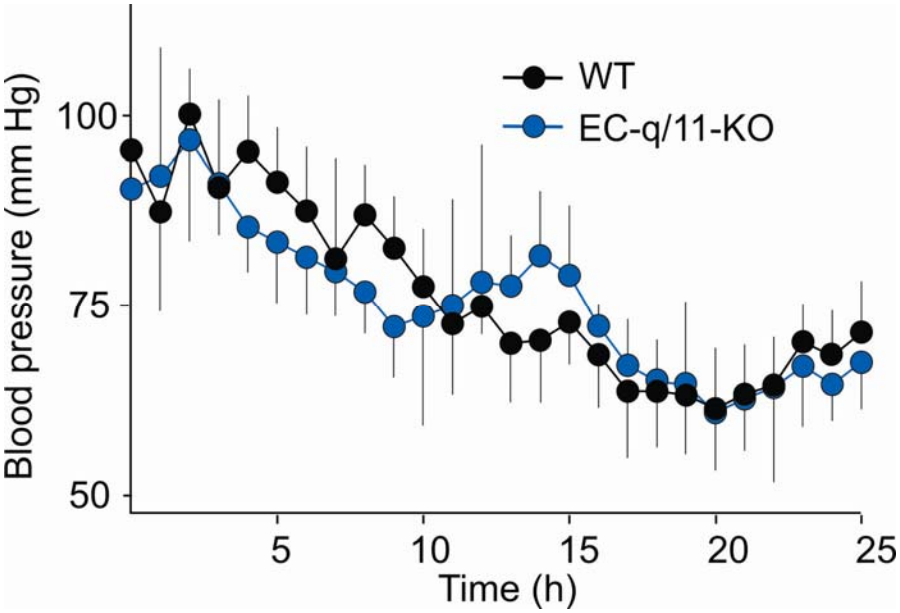

Figure 21. Role of endothelial G_q/G_{11} in endotoxic shock. 3 wild-type (WT) and EC-Gα_q/Gα_{11}-KO mice were injected i.p. with 80 µg/g LPS, and the blood pressure was monitored telemetrically for 25 h. Shown are mean values ± S.D.

7.8 Leukocyte rolling is reduced in EC- Gα_q/Gα_{11}-KO mice

To study trauma induced leukocyte rolling and adhesion I prepared cremaster muscles from wild type and EC-Gα_q/Gα_{11}-KO mice as described [172]. I then observed leukocyte rolling in the venules of cremaster muscle by intravital microscopy. Venules with diameters between 20 and 40 µm were analyzed. As shown in Figure 22 A, leukocyte rolling was reduced by about 35 % in EC-Gα_q/Gα_{11}-KO mice compared to wild type mice. After P-selectin antibody (RB40) injection leukocyte rolling was blocked as expected (Figure 22 A). We also analyzed individual leukocyte rolling velocities (mm/s) and counted adherent leukocytes before and after RB40 administration in the venules of cremaster muscles from EC-Gα_q/Gα_{11}-KO mice and wild-type mice. We did not observe significant difference in these parameters between EC-Gα_q/Gα_{11}-KO mice and wild-type mice. Adhesion was slightly but not significantly reduced in EC-Gα_q/Gα_{11}-KO mice before RB40

administration. After RB40 injection EC-Gα_q/Gα_{11}-KO mice showed reduced adhesion compared to wild-type mice (Figure 22 B and C).

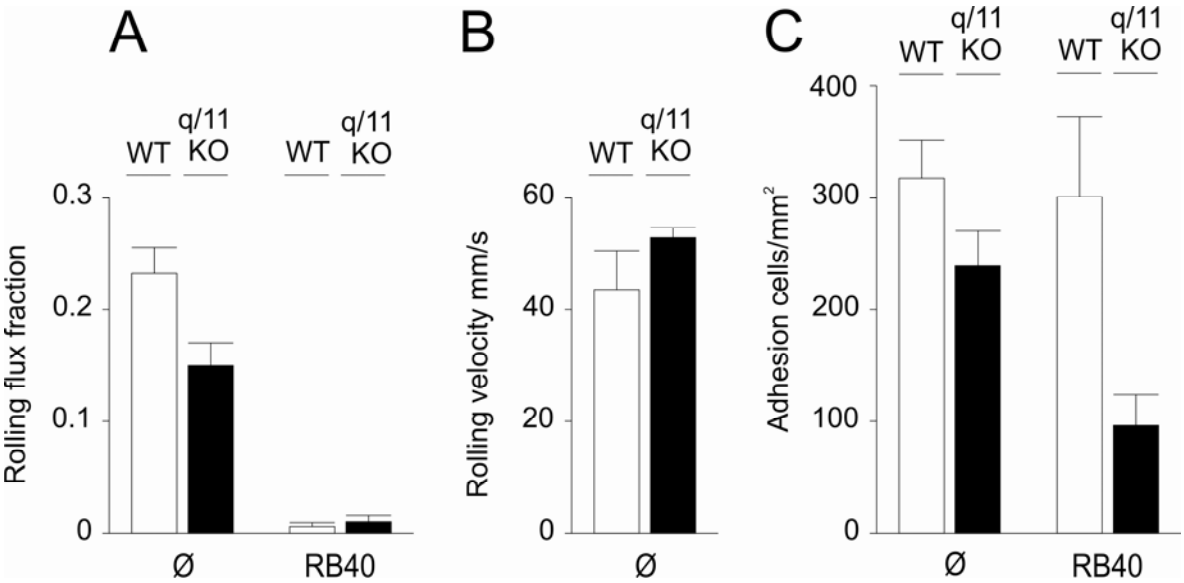

Figure 22. Leukocyte rolling and adhesion in the cremaster muscles of EC-Gα_q/Gα_{11}-KO and wild-type mice. Shown is the rolling flux fraction before and after RB40 administration (A), rolling velocity (B) and adhesion of leukocytes before and after RB40 administration (C). Data shown are means ± s.e.m.

8 DISCUSSION

Mediators acting via G-protein coupled receptors play an important role in the regulation of endothelial functions. Many inflammatory mediators, such as histamine, thrombin, and PAF, are known to act on receptors coupled to $G\alpha_{q/11}$- and $G\alpha_{12/13}$. To date it has not been possible to analyze $G_{q/11}$- and $G_{12/13}$-mediated signalling pathways *in vivo* in the endothelium of adult mice, due to the severe phenotype and early death of $G\alpha_{q/11}$-deficient mice, and embryonic lethality of $G\alpha_{12/13}$-deficient mice [30, 34]. To circumvent this problem, I crossed an inducible endothelial cell specific Tie-2 Cre-transgenic mouse line with mice carrying floxed alleles of the genes encoding $G\alpha_q$ (*Gnaq*) or $G\alpha_{13}$ (*Gna13*), and null alleles of the genes encoding $G\alpha_{11}$ (*Gna11*) or $G\alpha_{12}$ (*Gna12*). In order to analyze Cre-recombination, I also crossed Tie-2 Cre-transgenic mice with ROSA-26-LacZ reporter mice. The Tie-$2^{+/-}$, ROSA-26-$LacZ^{+/-}$ offspring from these matings were treated with tamoxifen or carrier solution. After induction of Cre-recombination, I observed endothelial cell specific expression of Cre- recombinase in various organs as verified by detection of β-galactosidase activity on cryosections. However, immune cells, aorta, and endothelial cells in the brain were not recombined. Non-inducible Tie-1 and Tie-2 Cre-mouse lines were generated and described before [180-182]. *Tie-1* and *Tie-2* are vascular endothelium specific receptor tyrosine kinases that are important for formation of new blood vessels [183], and are expressed in endothelial cells as early as at E8 [184]. Common feature of these non-inducible Cre-mouse lines is the expression of Cre-recombinase also in a population of hematopoietic cells. This is not surprising, since *Tie-1* and *Tie-2* are expressed in hemangioblasts, common progenitors of endothelial and blood cells [185]. Obviously, the Cre expression in hematopoietic cells can be avoided by using inducible Cre/loxP system [186], which was confirmed by expression studies in Tie-

2 Cre-mice used in this project. Non-inducible Tie-1 and Tie-2 Cre-mouse lines, as well as previously characterized inducible Tie-2 Cre-mice [186] all show Cre-recombination in the capillaries of the brain, which is inconsistent with my results. The reason behind this difference could be the early onset of the promoter in the non-inducible Tie-1 and Tie-2 mouse lines, or different induction scheme used in the inducible Tie-2 mouse line. Tamoxifen was administered in the food for induction period of 5 weeks, while I administered tamoxifen by i.p. injection for 5 days. The lack of recombination that I observed in the brain, could possibly be explained by the fact that tamoxifen might not reach the brain in sufficient concentration with this induction scheme. In contrast to my results, the non-inducible Tie-1 and Tie-2 Cre-mice also express Cre-recombinase in adult aorta. I observed Cre-recombination in all endothelial cells including the aorta in E14.5 embryos induced with tamoxifen at E8.5-E9.5, which is consistent with the Cre-expression data from the non-inducible Cre-mouse lines. Why the induction of Cre-recombination in the adult aorta was not successful is unclear.

Endothelium specific $G\alpha_{q/11}$- and $G\alpha_{12/13}$-deficient mice showed no obvious defects when unchallenged and the basal blood pressure of the mice was unaffected. When we challenged endothelial specific $G\alpha_{q/11}$-deficient mice with i.v. injection of histamine, we observed reduced hypotensive response in comparison to WT or $G\alpha_{12/13}$-deficient mice. This indicated that although $G\alpha_{q/11}$-mediated signalling did not play a role in regulation of endothelial functions under physiological conditions, it had an important role in the regulation of endothelial functions when mice were challenged by inflammation or anaphylaxis. However, we did not test if endothelium specific $G\alpha_{q/11}$- and $G\alpha_{12/13}$-deficieny affected the function of endothelium under physiological challenge such as exercise or shear stress. $G\alpha_{13}$ was shown to be essential for the normal development of vascular system during

embryonic angiogenesis [30, 31]. The formation of blood vessels during embryogenesis can be divided into two processes: differentiation of progenitor cells to endothelial cells (vasculogenesis) and subsequent growth, migration, and remodelling of endothelial cells (angiogenesis) [187]. Vasculogenesis was not affected by $G\alpha_{13}$-deficiency, but the defect occurred during early angiogenesis, indicating that $G\alpha_{13}$ was necessary for remodelling of vascular system [30]. In addition, $G\alpha_{13}$-deficient fibroblasts were unable to migrate when stimulated with thrombin, and $G\alpha_{13}$-deficient endothelial cells could not form networks of cords and tubes on Matrigel [30, 31]. This suggested that $G\alpha_{13}$ probably mediates the process of vascular remodelling during embryogenesis, but the role of it in adult angiogenesis remains undefined. In adults new blood vessels are formed only through angiogenesis, which takes place for instance during wound healing, in tumours, and in the development of "*corpus luteum*" during female reproductive cycle. $G\alpha_{12/13}$-deficiency did not affect the fertility of the female mice, thus the angiogenesis in the ovaries was obviously not impaired. The role of $G\alpha_{12/13}$-mediated signalling in the tumour angiogenesis remains to be analyzed.

The opening of the endothelial barrier requires contraction of the cells and disruption of cell-cell contacts. It can be stimulated by various inflammatory mediators such as histamine, LPA, or PAF [38, 61]. The contraction of the endothelial cells as well as smooth muscle cells is initiated by the phosphorylation of MLC. This process is dually regulated by Ca^{2+} dependent activation of MLC kinase [64] and by Ca^{2+} independent, RhoA/Rho kinase mediated deactivation of MLC phosphatase [65]. It is believed that the Ca^{2+} dependent pathway is activated by receptor coupling to $G\alpha_{q/11}$, and the Ca^{2+} independent pathway by receptors coupled to $G\alpha_{12/13}$ [188]. The experiments in mouse primary endothelial cells revealed an important role for $G\alpha_{q/11}$ signalling in phosphorylation of MLC. In the

absence of $G\alpha_{q/11}$, MLC phosphorylation in primary endothelial cells was abrogated. As expected, endothelial $G\alpha_{q/11}$- and $G\alpha_{12/13}$-deficieny resulted in blunted IP_3 production and RhoA activation, respectively. Lack of $G\alpha_{12/13}$ resulted in a reduced and more transient MLC phosphorylation, even in the absence of RhoA activation. In endothelial cells derived from human umbilical vein MLC phosphorylation was shown to reach the maximum 2 minutes after thrombin stimulation, and a reversal or slightly elevated phosphorylation was seen 5 minutes after thrombin stimulation [65]. Primary mouse endothelial cells stimulated with thrombin showed maximum MLC phosphorylation at 3 minutes, which was consistent with the previous study. However, we still saw moderately elevated phosphorylation at 10 minutes in WT cells, whereas the MLC phosphorylation in $G\alpha_{12/13}$ –deficient cells was back to basal values after 10 minutes. These data from *in vitro* MLC phosphorylation studies were consistent with the *in vivo* findings. In local permeability assay the extravasation of plasma could be determined with help of Evans blue dye [170]. $G\alpha_{q/11}$–deficient mice showed reduced plasma extravasation in response to stimulation with histamine, LPA, PAF, and PAR-1 peptide, as well as in a model of local anaphylaxis. In contrast $G\alpha_{12/13}$ –deficient mice reacted to these inflammatory stimuli like WT mice. Elevated hematocrit is one of the signs of anaphylactic shock; however the hematocrit was unchanged in $G\alpha_{q/11}$–deficient mice in a model of passive anaphylaxis, while it was significantly increased in WT and $G\alpha_{12/13}$–deficient mice. This indicated that the opening of the endothelial barrier did not occur in $G\alpha_{q/11}$–deficient mice in response to anaphylactic challenge. These *in vitro* and *in vivo* data suggest that $G\alpha_{q/11}$ is required for the opening of the endothelial barrier in response to different inflammatory stimuli and during anaphylactic reaction, while the role of $G\alpha_{12/13}$ appears to be less important. A recent study supported the role of $G\alpha_{q/11}$ in opening of the endothelial barrier [189].

Life-threatening anaphylactic shock can be caused by bee stings, food, or antibiotics. Its pathophysiology involves diverse signalling pathways and affects various organs like the heart, blood vessels, immune cells, and bronchial system [153]. When $G\alpha_{q/11}$–deficient mice were injected i.v. with histamine, the hypotensive response of the knock-out mice was reduced and short lasting in comparison to WT or $G\alpha_{12/13}$–deficient mice. PAF caused only small and transient drop in body temperature, and the $G\alpha_{q/11}$–deficient mice were protected from PAF induced shock and the fatal consequences of it. The vasodilator NO is generated during anaphylactic reaction, but its source has been unclear and the role controversial [91, 158, 159]. It has been generally thought that inducible iNOS mediates endotoxic as well as anaphylactic shock [163, 164]. A recent study in $eNOS^{-/-}$ mice suggested a role for eNOS rather than iNOS produced NO in anaphylactic shock [159]. However, the expression of eNOS is not restricted to endothelium. For instance macrophages express eNOS, and could be involved in anaphylaxis, thus leaving the origin of eNOS unclear [175]. The data from two anaphylaxis models used in this study support the suggested role for endothelium originating eNOS in anaphylactic shock. Endothelial cell specific $G\alpha_{q/11}$-deficient mice were protected from anaphylactic shock like $eNOS^{-/-}$ mice, and $G\alpha_{q/11}$-deficient mouse primary pulmonary endothelial cells failed to produce NO in response to thrombin and PAF stimulation. $G\alpha_{11}$ alone was not sufficient to protect mice from the fatal outcome of anaphylactic shock, but the $G\alpha_{11}^{-/-}$ mice showed an intermediate phenotype with 20 % (2/10) mice surviving the anaphylactic challenge. The absence of Cre-recombination in immune cells ruled out the possible involvement of immune cell derived eNOS in this study. NO has been suggested to play an important role during endotoxic shock, and to affect the occurrence of death [163, 179]. Nevertheless, eNOS- or iNOS- deficiency did not prevent the fatal consequences of endotoxic shock in mice [109]. Endothelial

$G\alpha_{q/11}$-deficiency was not protective in endotoxic shock, but the blood pressure and survival of the $G\alpha_{q/11}$-deficient mice were similar in comparison to WT and $G\alpha_{12/13}$-deficient mice. LPS induced endotoxic shock has been shown to be mediated by another signalling pathway involving the members of the Toll-like receptor family [190]. Thus these data suggest that endothelial $G\alpha_{q/11}$ is crucially required for anaphylaxis but does not play a role in endotoxic shock.

Leukocytes are recruited to the inflamed tissue by mechanisms involving leukocyte rolling, adhesion, and transmigration [134]. These processes are mediated by cytokine/chemokine signalling and leukocyte-endothelial interactions via various cell surface-expressed adhesion molecules [133]. In this study I employed intravital microscopy to observe trauma induced leukocyte rolling in the mouse cremaster muscle. Endothelial $G\alpha_{q/11}$-deficiency reduced leukocyte rolling by about 35 % in the venules of cremaster muscle in response to trauma-induced inflammation. The adhesion of leukocytes was slightly but not significantly reduced. Initiation of leukocyte rolling is mainly dependent on release of histamine [191], which triggers the rapid exposure of P-selectin on the surface of endothelial cells [192], but does not involve NO-dependent pathway [191]. The contribution of histamine to the leukocyte rolling is about 48 % [193]. Thus reduced leukocyte rolling in the $G\alpha_{q/11}$-deficienct mice was likely due to the inability of histamine, whose receptor couples to $G_{q/11}$, to exert its functions via the histamine receptor. These results support the role for Ca^{2+} signalling in leukocyte recruitment [148]. Reduction of endothelial MLCK activation was shown to significantly decrease leukocyte migration [61, 149, 150]. Whether the reduced leukocyte rolling and adhesion lead to reduced leukocyte transmigration in the $G\alpha_{q/11}$-deficienct mice was not determined in this study. The involvement of endothelial cell specific $G\alpha_{q/11}$-deficieny in later steps of leukocyte recruitment (leukocyte transmigration) remains to be elucidated.

In this study I investigated the roles of $G_{q/11}$- and $G_{12/13}$- mediated signalling pathways in the endothelium under physiological and pathophysiological conditions *in vivo* and *in vitro*. I was able to show that opening of endothelial barrier as well as anaphylactic shock required endothelial $G\alpha_{q/11}$, while $G\alpha_{12/13}$ seemed to be less important. This study provided new information on the contribution of individual G-protein-mediated signalling pathways in the regulation of endothelial functions, and added to the better understanding of vascular functions in general. Blocking the $G_{q/11}$-mediated signalling pathway could be an interesting option to prevent or treat anaphylactic shock in a clinical setting. Since PAF-receptor deficiency or PAF antagonists were successful in blocking anaphylaxis in mice [156, 157], the use of PAF antagonists together with H1-receptor blockers was considered as a promising therapy for anaphylaxis in human. Several PAF antagonists were developed [194, 195], but they proved to be inefficient in prevention or therapy of anaphylaxis in humans. PAF, histamine, and other inflammatory mediators all act on the same $G_{q/11}$-mediated signalling pathway. Therefore blocking one of the many receptors may not be sufficient, but blocking the signalling pathway somewhere downstream may be more efficacious.

9 REFERENCES

1. Augustin, H.G., D.H. Kozian, and R.C. Johnson, *Differentiation of endothelial cells: analysis of the constitutive and activated endothelial cell phenotypes.* Bioessays, 1994. **16**(12): p. 901-6.

2. Fishman, A.P., *Endothelium: a distributed organ of diverse capabilities.* Ann N Y Acad Sci, 1982. **401**: p. 1-8.

3. Wojciak-Stothard, B. and A.J. Ridley, *Rho GTPases and the regulation of endothelial permeability.* Vascul Pharmacol, 2002. **39**(4-5): p. 187-99.

4. Birnbaumer, L., *Receptor-to-effector signaling through G proteins: roles for beta gamma dimers as well as alpha subunits.* Cell, 1992. **71**(7): p. 1069-72.

5. Neer, E.J., *Heterotrimeric G proteins: organizers of transmembrane signals.* Cell, 1995. **80**(2): p. 249-57.

6. Hamm, H.E., *The many faces of G protein signaling.* J Biol Chem, 1998. **273**(2): p. 669-72.

7. Hepler, J.R. and A.G. Gilman, *G proteins.* Trends Biochem Sci, 1992. **17**(10): p. 383-7.

8. Simon, M.I., M.P. Strathmann, and N. Gautam, *Diversity of G proteins in signal transduction.* Science, 1991. **252**(5007): p. 802-8.

9. Wettschureck, N. and S. Offermanns, *Mammalian G proteins and their cell type specific functions.* Physiol Rev, 2005. **85**(4): p. 1159-204.

10. Offermanns, S., *G-proteins as transducers in transmembrane signalling.* Prog Biophys Mol Biol, 2003. **83**(2): p. 101-30.

11. Exton, J.H., *Regulation of phosphoinositide phospholipases by hormones, neurotransmitters, and other agonists linked to G proteins.* Annu Rev Pharmacol Toxicol, 1996. **36**: p. 481-509.

12. Rhee, S.G., *Regulation of phosphoinositide-specific phospholipase C.* Annu Rev Biochem, 2001. **70**: p. 281-312.

13. Offermanns, S., et al., *Gq and G11 are concurrently activated by bombesin and vasopressin in Swiss 3T3 cells.* FEBS Lett, 1994. **349**(2): p. 201-4.

14. Wange, R.L., et al., *Photoaffinity labeling of two rat liver plasma membrane proteins with [32P]gamma-azidoanilido GTP in response to vasopressin. Immunologic identification as alpha subunits of the Gq class of G proteins.* J Biol Chem, 1991. **266**(18): p. 11409-12.

15. Zywietz, A., et al., *Pleiotropic effects of Pasteurella multocida toxin are mediated by Gq-dependent and -independent mechanisms. involvement of Gq but not G11.* J Biol Chem, 2001. **276**(6): p. 3840-5.

16. Offermanns, S., et al., *Impaired motor coordination and persistent multiple climbing fiber innervation of cerebellar Purkinje cells in mice lacking Galphaq.* Proc Natl Acad Sci U S A, 1997. **94**(25): p. 14089-94.

17. Offermanns, S., et al., *Embryonic cardiomyocyte hypoplasia and craniofacial defects in G alpha q/G alpha 11-mutant mice.* EMBO J, 1998. **17**(15): p. 4304-12.

18. Wettschureck, N., et al., *Absence of pressure overload induced myocardial hypertrophy after conditional inactivation of Galphaq/Galpha11 in cardiomyocytes.* Nat Med, 2001. **7**(11): p. 1236-40.

19. Davignon, I., et al., *Normal hematopoiesis and inflammatory responses despite discrete signaling defects in Galpha15 knockout mice.* Mol Cell Biol, 2000. **20**(3): p. 797-804.

20. Strathmann, M.P. and M.I. Simon, *G alpha 12 and G alpha 13 subunits define a fourth class of G protein alpha subunits.* Proc Natl Acad Sci U S A, 1991. **88**(13): p. 5582-6.

21. Dhanasekaran, N. and J.M. Dermott, *Signaling by the G12 class of G proteins.* Cell Signal, 1996. **8**(4): p. 235-45.

22. Hooley, R., et al., *G alpha 13 stimulates Na+-H+ exchange through distinct Cdc42-dependent and RhoA-dependent pathways.* J Biol Chem, 1996. **271**(11): p. 6152-8.

23. Plonk, S.G., S.K. Park, and J.H. Exton, *The alpha-subunit of the heterotrimeric G protein G13 activates a phospholipase D isozyme by a pathway requiring Rho family GTPases.* J Biol Chem, 1998. **273**(9): p. 4823-6.

24. Buhl, A.M., et al., *G alpha 12 and G alpha 13 stimulate Rho-dependent stress fiber formation and focal adhesion assembly.* J Biol Chem, 1995. **270**(42): p. 24631-4.

25. Fukuhara, S., H. Chikumi, and J.S. Gutkind, *RGS-containing RhoGEFs: the missing link between transforming G proteins and Rho?* Oncogene, 2001. **20**(13): p. 1661-8.

26. Hart, M.J., et al., *Direct stimulation of the guanine nucleotide exchange activity of p115 RhoGEF by Galpha13.* Science, 1998. **280**(5372): p. 2112-4.

27. Suzuki, N., et al., *Galpha 12 activates Rho GTPase through tyrosine-phosphorylated leukemia-associated RhoGEF.* Proc Natl Acad Sci U S A, 2003. **100**(2): p. 733-8.

28. Meigs, T.E., et al., *Galpha12 and Galpha13 negatively regulate the adhesive functions of cadherin.* J Biol Chem, 2002. **277**(27): p. 24594-600.

29. Meigs, T.E., et al., *Interaction of Galpha 12 and Galpha 13 with the cytoplasmic domain of cadherin provides a mechanism for beta -catenin release.* Proc Natl Acad Sci U S A, 2001. **98**(2): p. 519-24.

30. Offermanns, S., et al., *Vascular system defects and impaired cell chemokinesis as a result of Galpha13 deficiency.* Science, 1997. **275**(5299): p. 533-6.

31. Ruppel, K.M., et al., *Essential role for Galpha13 in endothelial cells during embryonic development.* Proc Natl Acad Sci U S A, 2005. **102**(23): p. 8281-6.

32. Connolly, A.J., et al., *Role of the thrombin receptor in development and evidence for a second receptor.* Nature, 1996. **381**(6582): p. 516-9.

33. Griffin, C.T., et al., *A role for thrombin receptor signaling in endothelial cells during embryonic development.* Science, 2001. **293**(5535): p. 1666-70.

34. Gu, J.L., et al., *Interaction of G alpha(12) with G alpha(13) and G alpha(q) signaling pathways.* Proc Natl Acad Sci U S A, 2002. **99**(14): p. 9352-7.

35. Bazzoni, G. and E. Dejana, *Endothelial cell-to-cell junctions: molecular organization and role in vascular homeostasis.* Physiol Rev, 2004. **84**(3): p. 869-901.

36. Rubin, L.L. and J.M. Staddon, *The cell biology of the blood-brain barrier.* Annu Rev Neurosci, 1999. **22**: p. 11-28.

37. Dejana, E., M. Corada, and M.G. Lampugnani, *Endothelial cell-to-cell junctions.* FASEB J, 1995. **9**(10): p. 910-8.

38. Mehta, D. and A.B. Malik, *Signaling mechanisms regulating endothelial permeability.* Physiol Rev, 2006. **86**(1): p. 279-367.

39. Lampugnani, M.G., et al., *The molecular organization of endothelial cell to cell junctions: differential association of plakoglobin, beta-catenin, and alpha-catenin with vascular endothelial cadherin (VE-cadherin).* J Cell Biol, 1995. **129**(1): p. 203-17.

40. Breier, G., et al., *Molecular cloning and expression of murine vascular endothelial-cadherin in early stage development of cardiovascular system.* Blood, 1996. **87**(2): p. 630-41.

41. Carmeliet, P., et al., *Targeted deficiency or cytosolic truncation of the VE-cadherin gene in mice impairs VEGF-mediated endothelial survival and angiogenesis.* Cell, 1999. **98**(2): p. 147-57.

42. Vittet, D., et al., *Targeted null-mutation in the vascular endothelial-cadherin gene impairs the organization of vascular-like structures in embryoid bodies.* Proc Natl Acad Sci U S A, 1997. **94**(12): p. 6273-8.

43. Cattelino, A., et al., *The conditional inactivation of the beta-catenin gene in endothelial cells causes a defective vascular pattern and increased vascular fragility.* J Cell Biol, 2003. **162**(6): p. 1111-22.

44. Wojciak-Stothard, B., et al., *Rho and Rac but not Cdc42 regulate endothelial cell permeability.* J Cell Sci, 2001. **114**(Pt 7): p. 1343-55.

45. Van Itallie, C.M. and J.M. Anderson, *Occludin confers adhesiveness when expressed in fibroblasts.* J Cell Sci, 1997. **110 (Pt 9)**: p. 1113-21.

46. Goodenough, D.A. and D.L. Paul, *Beyond the gap: functions of unpaired connexon channels.* Nat Rev Mol Cell Biol, 2003. **4**(4): p. 285-94.

47. Goodenough, D.A., J.A. Goliger, and D.L. Paul, *Connexins, connexons, and intercellular communication.* Annu Rev Biochem, 1996. **65**: p. 475-502.

48. van Rijen, H.V., et al., *Tumour necrosis factor alpha alters the expression of connexin43, connexin40, and connexin37 in human umbilical vein endothelial cells.* Cytokine, 1998. **10**(4): p. 258-64.

49. Van Rijen, H., et al., *Gap junctions in human umbilical cord endothelial cells contain multiple connexins.* Am J Physiol, 1997. **272**(1 Pt 1): p. C117-30.

50. Carter, T.D., et al., *Porcine aortic endothelial gap junctions: identification and permeation by caged InsP3.* J Cell Sci, 1996. **109 (Pt 7)**: p. 1765-73.

51. Carter, T.D. and D. Ogden, *Acetylcholine-stimulated changes of membrane potential and intracellular Ca2+ concentration recorded in endothelial cells in situ in the isolated rat aorta.* Pflugers Arch, 1994. **428**(5-6): p. 476-84.

52. Pepper, M.S., et al., *Junctional communication is induced in migrating capillary endothelial cells.* J Cell Biol, 1989. **109**(6 Pt 1): p. 3027-38.

53. Larson, D.M. and C.C. Haudenschild, *Junctional transfer in wounded cultures of bovine aortic endothelial cells.* Lab Invest, 1988. **59**(3): p. 373-9.

54. Cooper, C.D., et al., *Analysis of connexin phosphorylation sites.* Methods, 2000. **20**(2): p. 196-204.

55. Suarez, S. and K. Ballmer-Hofer, *VEGF transiently disrupts gap junctional communication in endothelial cells.* J Cell Sci, 2001. **114**(Pt 6): p. 1229-35.

56. Simon, A.M. and A.R. McWhorter, *Vascular abnormalities in mice lacking the endothelial gap junction proteins connexin37 and connexin40.* Dev Biol, 2002. **251**(2): p. 206-20.

57. Liao, Y., et al., *Endothelial cell-specific knockout of connexin 43 causes hypotension and bradycardia in mice.* Proc Natl Acad Sci U S A, 2001. **98**(17): p. 9989-94.

58. Dudek, S.M. and J.G. Garcia, *Cytoskeletal regulation of pulmonary vascular permeability.* J Appl Physiol, 2001. **91**(4): p. 1487-500.

59. Shasby, D.M., et al., *Role of endothelial cell cytoskeleton in control of endothelial permeability.* Circ Res, 1982. **51**(5): p. 657-61.

60. Phillips, P.G., et al., *Phallacidin prevents thrombin-induced increases in endothelial permeability to albumin.* Am J Physiol, 1989. **257**(3 Pt 1): p. C562-7.

61. Garcia, J.G., H.W. Davis, and C.E. Patterson, *Regulation of endothelial cell gap formation and barrier dysfunction: role of myosin light chain phosphorylation.* J Cell Physiol, 1995. **163**(3): p. 510-22.

62. Ellis, C.A., et al., *Time course of recovery of endothelial cell surface thrombin receptor (PAR-1) expression.* Am J Physiol, 1999. **276**(1 Pt 1): p. C38-45.

63. Vogel, S.M., et al., *Abrogation of thrombin-induced increase in pulmonary microvascular permeability in PAR-1 knockout mice.* Physiol Genomics, 2000. **4**(2): p. 137-145.

64. Wysolmerski, R.B. and D. Lagunoff, *Involvement of myosin light-chain kinase in endothelial cell retraction.* Proc Natl Acad Sci U S A, 1990. **87**(1): p. 16-20.

65. Aepfelbacher, M. and M. Essler, *Disturbance of endothelial barrier function by bacterial toxins and atherogenic mediators: a role for Rho/Rho kinase.* Cell Microbiol, 2001. **3**(10): p. 649-58.

66. Wettschureck, N. and S. Offermanns, *Rho/Rho-kinase mediated signaling in physiology and pathophysiology.* J Mol Med, 2002. **80**(10): p. 629-38.

67. van Nieuw Amerongen, G.P., et al., *Transient and prolonged increase in endothelial permeability induced by histamine and thrombin: role of protein kinases, calcium, and RhoA.* Circ Res, 1998. **83**(11): p. 1115-23.

68. van Nieuw Amerongen, G.P., et al., *Activation of RhoA by thrombin in endothelial hyperpermeability: role of Rho kinase and protein tyrosine kinases.* Circ Res, 2000. **87**(4): p. 335-40.

69. Lum, H. and A.B. Malik, *Regulation of vascular endothelial barrier function.* Am J Physiol, 1994. **267**(3 Pt 1): p. L223-41.

70. Moy, A.B., et al., *Histamine and thrombin modulate endothelial focal adhesion through centripetal and centrifugal forces.* J Clin Invest, 1996. **97**(4): p. 1020-7.

71. Clapham, D.E., *Calcium signaling.* Cell, 1995. **80**(2): p. 259-68.

72. Parekh, A.B. and R. Penner, *Store depletion and calcium influx.* Physiol Rev, 1997. **77**(4): p. 901-30.

73. Wysolmerski, R.B. and D. Lagunoff, *Regulation of permeabilized endothelial cell retraction by myosin phosphorylation.* Am J Physiol, 1991. **261**(1 Pt 1): p. C32-40.

74. Dejana, E., *Endothelial adherens junctions: implications in the control of vascular permeability and angiogenesis.* J Clin Invest, 1996. **98**(9): p. 1949-53.

75. Gao, X., et al., *Reversibility of increased microvessel permeability in response to VE-cadherin disassembly.* Am J Physiol Lung Cell Mol Physiol, 2000. **279**(6): p. L1218-25.

76. Sandoval, R., et al., *Ca(2+) signalling and PKCalpha activate increased endothelial permeability by disassembly of VE-cadherin junctions.* J Physiol, 2001. **533**(Pt 2): p. 433-45.

77. Tiruppathi, C., et al., *Impairment of store-operated Ca2+ entry in TRPC4(-/-) mice interferes with increase in lung microvascular permeability.* Circ Res, 2002. **91**(1): p. 70-6.

78. Sah, V.P., et al., *The role of Rho in G protein-coupled receptor signal transduction.* Annu Rev Pharmacol Toxicol, 2000. **40**: p. 459-89.

79. Bishop, A.L. and A. Hall, *Rho GTPases and their effector proteins.* Biochem J, 2000. **348 Pt 2**: p. 241-55.

80. Kimura, K., et al., *Regulation of myosin phosphatase by Rho and Rho-associated kinase (Rho-kinase).* Science, 1996. **273**(5272): p. 245-8.

81. Hirase, T., et al., *Regulation of tight junction permeability and occludin phosphorylation by Rhoa-p160ROCK-dependent and -independent mechanisms.* J Biol Chem, 2001. **276**(13): p. 10423-31.

82. Essler, M., et al., *Thrombin inactivates myosin light chain phosphatase via Rho and its target Rho kinase in human endothelial cells.* J Biol Chem, 1998. **273**(34): p. 21867-74.

83. Carbajal, J.M. and R.C. Schaeffer, Jr., *RhoA inactivation enhances endothelial barrier function.* Am J Physiol, 1999. **277**(5 Pt 1): p. C955-64.

84. Carbajal, J.M., et al., *ROCK mediates thrombin's endothelial barrier dysfunction.* Am J Physiol Cell Physiol, 2000. **279**(1): p. C195-204.

85. Alexander, J.S., *Rho, tyrosine kinase, Ca(2+), and junctions in endothelial hyperpermeability.* Circ Res, 2000. **87**(4): p. 268-71.

86. Stockton, R.A., E. Schaefer, and M.A. Schwartz, *p21-activated kinase regulates endothelial permeability through modulation of contractility.* J Biol Chem, 2004. **279**(45): p. 46621-30.

87. Gavard, J. and J.S. Gutkind, *VEGF controls endothelial-cell permeability by promoting the beta-arrestin-dependent endocytosis of VE-cadherin.* Nat Cell Biol, 2006. **8**(11): p. 1223-34.

88. Kouklis, P., et al., *Cdc42 regulates the restoration of endothelial barrier function.* Circ Res, 2004. **94**(2): p. 159-66.

89. Wildenberg, G.A., et al., *p120-catenin and p190RhoGAP regulate cell-cell adhesion by coordinating antagonism between Rac and Rho.* Cell, 2006. **127**(5): p. 1027-39.

90. Furchgott, R.F. and J.V. Zawadzki, *The obligatory role of endothelial cells in the relaxation of arterial smooth muscle by acetylcholine.* Nature, 1980. **288**(5789): p. 373-6.

91. Palmer, R.M., A.G. Ferrige, and S. Moncada, *Nitric oxide release accounts for the biological activity of endothelium-derived relaxing factor.* Nature, 1987. **327**(6122): p. 524-6.

92. Ignarro, L.J., et al., *Endothelium-derived relaxing factor produced and released from artery and vein is nitric oxide.* Proc Natl Acad Sci U S A, 1987. **84**(24): p. 9265-9.

93. Ignarro, L.J., et al., *Endothelium-derived relaxing factor from pulmonary artery and vein possesses pharmacologic and chemical properties identical to those of nitric oxide radical.* Circ Res, 1987. **61**(6): p. 866-79.

94. Cauwels, A., *Nitric oxide in shock.* Kidney Int, 2007. **72**(5): p. 557-65.

95. Fleming, I. and R. Busse, *Molecular mechanisms involved in the regulation of the endothelial nitric oxide synthase.* Am J Physiol Regul Integr Comp Physiol, 2003. **284**(1): p. R1-12.

96. Huang, P.L., et al., *Hypertension in mice lacking the gene for endothelial nitric oxide synthase.* Nature, 1995. **377**(6546): p. 239-42.

97. Rudic, R.D., et al., *Direct evidence for the importance of endothelium-derived nitric oxide in vascular remodeling.* J Clin Invest, 1998. **101**(4): p. 731-6.

98. Murohara, T., et al., *Nitric oxide synthase modulates angiogenesis in response to tissue ischemia.* J Clin Invest, 1998. **101**(11): p. 2567-78.

99. Predescu, D., et al., *Constitutive eNOS-derived nitric oxide is a determinant of endothelial junctional integrity.* Am J Physiol Lung Cell Mol Physiol, 2005. **289**(3): p. L371-81.

100. Busse, R. and A. Mulsch, *Calcium-dependent nitric oxide synthesis in endothelial cytosol is mediated by calmodulin.* FEBS Lett, 1990. **265**(1-2): p. 133-6.

101. Luckhoff, A., et al., *Differential role of extra- and intracellular calcium in the release of EDRF and prostacyclin from cultured endothelial cells.* Br J Pharmacol, 1988. **95**(1): p. 189-96.

102. Ayajiki, K., et al., *Intracellular pH and tyrosine phosphorylation but not calcium determine shear stress-induced nitric oxide production in native endothelial cells.* Circ Res, 1996. **78**(5): p. 750-8.

103. Dimmeler, S., et al., *Activation of nitric oxide synthase in endothelial cells by Akt-dependent phosphorylation.* Nature, 1999. **399**(6736): p. 601-5.

104. Fulton, D., et al., *Regulation of endothelium-derived nitric oxide production by the protein kinase Akt.* Nature, 1999. **399**(6736): p. 597-601.

105. Fleming, I., et al., *Ca2+-independent activation of the endothelial nitric oxide synthase in response to tyrosine phosphatase inhibitors and fluid shear stress.* Circ Res, 1998. **82**(6): p. 686-95.

106. Motley, E.D., et al., *Mechanism of endothelial nitric oxide synthase phosphorylation and activation by thrombin.* Hypertension, 2007. **49**(3): p. 577-83.

107. Fleming, I., et al., *Phosphorylation of Thr(495) regulates Ca(2+)/calmodulin-dependent endothelial nitric oxide synthase activity.* Circ Res, 2001. **88**(11): p. E68-75.

108. Kim, F., B. Gallis, and M.A. Corson, *TNF-alpha inhibits flow and insulin signaling leading to NO production in aortic endothelial cells.* Am J Physiol Cell Physiol, 2001. **280**(5): p. C1057-65.

109. Shesely, E.G., et al., *Elevated blood pressures in mice lacking endothelial nitric oxide synthase.* Proc Natl Acad Sci U S A, 1996. **93**(23): p. 13176-81.

110. Thiemermann, C. and J. Vane, *Inhibition of nitric oxide synthesis reduces the hypotension induced by bacterial lipopolysaccharides in the rat in vivo.* Eur J Pharmacol, 1990. **182**(3): p. 591-5.

111. Feihl, F., B. Waeber, and L. Liaudet, *Is nitric oxide overproduction the target of choice for the management of septic shock?* Pharmacol Ther, 2001. **91**(3): p. 179-213.

112. Taylor, S.G. and A.H. Weston, *Endothelium-derived hyperpolarizing factor: a new endogenous inhibitor from the vascular endothelium.* Trends Pharmacol Sci, 1988. **9**(8): p. 272-4.

113. McGuire, J.J., H. Ding, and C.R. Triggle, *Endothelium-derived relaxing factors: a focus on endothelium-derived hyperpolarizing factor(s).* Can J Physiol Pharmacol, 2001. **79**(6): p. 443-70.

114. Kohler, R. and J. Hoyer, *The endothelium-derived hyperpolarizing factor: insights from genetic animal models.* Kidney Int, 2007. **72**(2): p. 145-50.

115. Edwards, G., et al., *K+ is an endothelium-derived hyperpolarizing factor in rat arteries.* Nature, 1998. **396**(6708): p. 269-72.

116. Fisslthaler, B., et al., *Cytochrome P450 2C is an EDHF synthase in coronary arteries.* Nature, 1999. **401**(6752): p. 493-7.

117. Campbell, W.B. and J.R. Falck, *Arachidonic acid metabolites as endothelium-derived hyperpolarizing factors.* Hypertension, 2007. **49**(3): p. 590-6.

118. Faraci, F.M., et al., *Arachidonate dilates basilar artery by lipoxygenase-dependent mechanism and activation of K(+) channels.* Am J Physiol Regul Integr Comp Physiol, 2001. **281**(1): p. R246-53.

119. Bolotina, V.M., et al., *Nitric oxide directly activates calcium-dependent potassium channels in vascular smooth muscle.* Nature, 1994. **368**(6474): p. 850-3.

120. Ellis, A. and C.R. Triggle, *Endothelium-derived reactive oxygen species: their relationship to endothelium-dependent hyperpolarization and vascular tone.* Can J Physiol Pharmacol, 2003. **81**(11): p. 1013-28.

121. Griffith, T.M., et al., *cAMP facilitates EDHF-type relaxations in conduit arteries by enhancing electrotonic conduction via gap junctions.* Proc Natl Acad Sci U S A, 2002. **99**(9): p. 6392-7.

122. Chauhan, S.D., et al., *Release of C-type natriuretic peptide accounts for the biological activity of endothelium-derived hyperpolarizing factor.* Proc Natl Acad Sci U S A, 2003. **100**(3): p. 1426-31.

123. Sandow, S.L. and C.E. Hill, *Incidence of myoendothelial gap junctions in the proximal and distal mesenteric arteries of the rat is suggestive of a role in endothelium-derived hyperpolarizing factor-mediated responses.* Circ Res, 2000. **86**(3): p. 341-6.

124. Shimokawa, H., et al., *The importance of the hyperpolarizing mechanism increases as the vessel size decreases in endothelium-dependent relaxations in rat mesenteric circulation.* J Cardiovasc Pharmacol, 1996. **28**(5): p. 703-11.

125. Mulvany, M.J. and C. Aalkjaer, *Structure and function of small arteries.* Physiol Rev, 1990. **70**(4): p. 921-61.

126. Taddei, S., et al., *Identification of a cytochrome P450 2C9-derived endothelium-derived hyperpolarizing factor in essential hypertensive patients.* J Am Coll Cardiol, 2006. **48**(3): p. 508-15.

127. Fisslthaler, B., et al., *Cyclic stretch enhances the expression and activity of coronary endothelium-derived hyperpolarizing factor synthase.* Hypertension, 2001. **38**(6): p. 1427-32.

128. Bussemaker, E., et al., *Aged spontaneously hypertensive rats exhibit a selective loss of EDHF-mediated relaxation in the renal artery.* Hypertension, 2003. **42**(4): p. 562-8.

129. Gschwend, S., et al., *Impaired coronary endothelial function in a rat model of spontaneous albuminuria.* Kidney Int, 2002. **62**(1): p. 181-91.

130. Burnham, M.P., I.T. Johnson, and A.H. Weston, *Impaired small-conductance Ca2+-activated K+ channel-dependent EDHF responses in Type II diabetic ZDF rats.* Br J Pharmacol, 2006. **148**(4): p. 434-41.

131. Scotland, R.S., et al., *Investigation of vascular responses in endothelial nitric oxide synthase/cyclooxygenase-1 double-knockout mice: key role for endothelium-derived hyperpolarizing factor in the regulation of blood pressure in vivo.* Circulation, 2005. **111**(6): p. 796-803.

132. Rao, R.M., et al., *Endothelial-dependent mechanisms of leukocyte recruitment to the vascular wall.* Circ Res, 2007. **101**(3): p. 234-47.

133. Wagner, J.G. and R.A. Roth, *Neutrophil migration mechanisms, with an emphasis on the pulmonary vasculature.* Pharmacol Rev, 2000. **52**(3): p. 349-74.

134. Springer, T.A., *Traffic signals for lymphocyte recirculation and leukocyte emigration: the multistep paradigm.* Cell, 1994. **76**(2): p. 301-14.

135. Butcher, E.C., *Leukocyte-endothelial cell recognition: three (or more) steps to specificity and diversity.* Cell, 1991. **67**(6): p. 1033-6.

136. Ley, K., et al., *Sequential contribution of L- and P-selectin to leukocyte rolling in vivo.* J Exp Med, 1995. **181**(2): p. 669-75.

137. Kunkel, E.J. and K. Ley, *Distinct phenotype of E-selectin-deficient mice. E-selectin is required for slow leukocyte rolling in vivo.* Circ Res, 1996. **79**(6): p. 1196-204.

138. Jung, U., et al., *Gene-targeted mice reveal importance of L-selectin-dependent rolling for neutrophil adhesion.* Am J Physiol, 1998. **274**(5 Pt 2): p. H1785-91.

139. Sperandio, M., *Selectins and glycosyltransferases in leukocyte rolling in vivo.* FEBS J, 2006. **273**(19): p. 4377-89.

140. Xia, L., et al., *P-selectin glycoprotein ligand-1-deficient mice have impaired leukocyte tethering to E-selectin under flow.* J Clin Invest, 2002. **109**(7): p. 939-50.

141. Yang, J., et al., *Targeted gene disruption demonstrates that P-selectin glycoprotein ligand 1 (PSGL-1) is required for P-selectin-mediated but not E-selectin-mediated neutrophil rolling and migration.* J Exp Med, 1999. **190**(12): p. 1769-82.

142. Norman, K.E., et al., *Leukocyte rolling in vivo is mediated by P-selectin glycoprotein ligand-1.* Blood, 1995. **86**(12): p. 4417-21.

143. Borges, E., et al., *The P-selectin glycoprotein ligand-1 is important for recruitment of neutrophils into inflamed mouse peritoneum.* Blood, 1997. **90**(5): p. 1934-42.

144. Moore, K.L., et al., *P-selectin glycoprotein ligand-1 mediates rolling of human neutrophils on P-selectin.* J Cell Biol, 1995. **128**(4): p. 661-71.

145. Sperandio, M., et al., *Severe impairment of leukocyte rolling in venules of core 2 glucosaminyltransferase-deficient mice.* Blood, 2001. **97**(12): p. 3812-9.

146. Adamson, P., et al., *Lymphocyte migration through brain endothelial cell monolayers involves signaling through endothelial ICAM-1 via a rho-dependent pathway.* J Immunol, 1999. **162**(5): p. 2964-73.

147. Greenwood, J., et al., *Intracellular domain of brain endothelial intercellular adhesion molecule-1 is essential for T lymphocyte-mediated signaling and migration.* J Immunol, 2003. **171**(4): p. 2099-108.

148. Huang, A.J., et al., *Endothelial cell cytosolic free calcium regulates neutrophil migration across monolayers of endothelial cells.* J Cell Biol, 1993. **120**(6): p. 1371-80.

149. Hixenbaugh, E.A., et al., *Stimulated neutrophils induce myosin light chain phosphorylation and isometric tension in endothelial cells.* Am J Physiol, 1997. **273**(2 Pt 2): p. H981-8.

150. Saito, H., et al., *Endothelial myosin light chain kinase regulates neutrophil migration across human umbilical vein endothelial cell monolayer.* J Immunol, 1998. **161**(3): p. 1533-40.

151. Kemp, S.F. and R.F. Lockey, *Anaphylaxis: a review of causes and mechanisms.* J Allergy Clin Immunol, 2002. **110**(3): p. 341-8.

152. Neugut, A.I., A.T. Ghatak, and R.L. Miller, *Anaphylaxis in the United States: an investigation into its epidemiology.* Arch Intern Med, 2001. **161**(1): p. 15-21.

153. Finkelman, F.D., *Anaphylaxis: lessons from mouse models.* J Allergy Clin Immunol, 2007. **120**(3): p. 506-15; quiz 516-7.

154. Compton, S.J., et al., *Restricted ability of human mast cell tryptase to activate proteinase-activated receptor-2 in rat aorta.* Can J Physiol Pharmacol, 2002. **80**(10): p. 987-92.

155. Ramachandran, R. and M.D. Hollenberg, *Proteinases and signalling: pathophysiological and therapeutic implications via PARs and more.* Br J Pharmacol, 2008. **153 Suppl 1**: p. S263-82.

156. Terashita, Z., et al., *Beneficial effects of (RS)-2-methoxy-3-(octadecylcarbamoyloxy)propyl 2-(3-thiazolio)ethyl phosphate, a specific PAF antagonist, in endotoxin and anaphylactic shock.* Adv Prostaglandin Thromboxane Leukot Res, 1985. **15**: p. 715-7.

157. Ishii, S., et al., *Impaired anaphylactic responses with intact sensitivity to endotoxin in mice lacking a platelet-activating factor receptor.* J Exp Med, 1998. **187**(11): p. 1779-88.

158. Mitsuhata, H., R. Shimizu, and M.M. Yokoyama, *Role of nitric oxide in anaphylactic shock.* J Clin Immunol, 1995. **15**(6): p. 277-83.

159. Cauwels, A., et al., *Anaphylactic shock depends on PI3K and eNOS-derived NO.* J Clin Invest, 2006. **116**(8): p. 2244-51.

160. Amir, S. and A.M. English, *An inhibitor of nitric oxide production, NG-nitro-L-arginine-methyl ester, improves survival in anaphylactic shock.* Eur J Pharmacol, 1991. **203**(1): p. 125-7.

161. Mitsuhata, H., et al., *Nitric oxide synthase inhibition is detrimental to cardiac function and promotes bronchospasm in anaphylaxis in rabbits.* Shock, 1995. **4**(2): p. 143-8.

162. Bellou, A., et al., *Constitutive nitric oxide synthase inhibition combined with histamine and serotonin receptor blockade improves the initial ovalbumin-induced arterial hypotension but decreases the survival time in brown norway rats anaphylactic shock.* Shock, 2003. **19**(1): p. 71-8.

163. Szabo, C. and C. Thiemermann, *Invited opinion: role of nitric oxide in hemorrhagic, traumatic, and anaphylactic shock and thermal injury.* Shock, 1994. **2**(2): p. 145-55.

164. Szabo, C., et al., *Platelet-activating factor contributes to the induction of nitric oxide synthase by bacterial lipopolysaccharide.* Circ Res, 1993. **73**(6): p. 991-9.

165. Sade, K., et al., *Expression of inducible nitric oxide synthase in a mouse model of anaphylaxis.* J Investig Allergol Clin Immunol, 2007. **17**(6): p. 379-85.

166. Moers, A., et al., *G13 is an essential mediator of platelet activation in hemostasis and thrombosis.* Nat Med, 2003. **9**(11): p. 1418-22.

167. Soriano, P., *Generalized lacZ expression with the ROSA26 Cre reporter strain.* Nat Genet, 1999. **21**(1): p. 70-1.

168. Fleming, I., et al., *Role of PECAM-1 in the shear-stress-induced activation of Akt and the endothelial nitric oxide synthase (eNOS) in endothelial cells.* J Cell Sci, 2005. **118**(Pt 18): p. 4103-11.

169. Fisslthaler, B., et al., *Inhibition of endothelial nitric oxide synthase activity by proline-rich tyrosine kinase 2 in response to fluid shear stress and insulin.* Circ Res, 2008. **102**(12): p. 1520-8.

170. Rogers, D.F., P. Boschetto, and P.J. Barnes, *Plasma exudation. Correlation between Evans blue dye and radiolabeled albumin in guinea pig airways in vivo.* J Pharmacol Methods, 1989. **21**(4): p. 309-15.

171. Wirth, A., et al., *G12-G13-LARG-mediated signaling in vascular smooth muscle is required for salt-induced hypertension.* Nat Med, 2008. **14**(1): p. 64-8.

172. Baez, S., *An open cremaster muscle preparation for the study of blood vessels by in vivo microscopy.* Microvasc Res, 1973. **5**(3): p. 384-94.

173. Norman, K.E., et al., *P-selectin glycoprotein ligand-1 supports rolling on E- and P-selectin in vivo.* Blood, 2000. **96**(10): p. 3585-91.

174. Kruth, H.S., *Lipoprotein cholesterol and atherosclerosis.* Curr Mol Med, 2001. **1**(6): p. 633-53.

175. Lowenstein, C.J. and T. Michel, *What's in a name? eNOS and anaphylactic shock.* J Clin Invest, 2006. **116**(8): p. 2075-8.

176. Indra, A.K., et al., *Temporally-controlled site-specific mutagenesis in the basal layer of the epidermis: comparison of the recombinase activity of the tamoxifen-inducible Cre-ER(T) and Cre-ER(T2) recombinases.* Nucleic Acids Res, 1999. **27**(22): p. 4324-7.

177. Braquet, P., P. Guinot, and C. Touvay, *The role of PAF-acether in anaphylaxis demonstrated with the use of the antagonist BN 52021.* Agents Actions Suppl, 1987. **21**: p. 97-117.

178. Vadas, P., et al., *Platelet-activating factor, PAF acetylhydrolase, and severe anaphylaxis.* N Engl J Med, 2008. **358**(1): p. 28-35.

179. Goode, H.F., et al., *Nitric oxide synthase activity is increased in patients with sepsis syndrome.* Clin Sci (Lond), 1995. **88**(2): p. 131-3.

180. Gustafsson, E., et al., *Tie-1-directed expression of Cre recombinase in endothelial cells of embryoid bodies and transgenic mice.* J Cell Sci, 2001. **114**(Pt 4): p. 671-6.

181. Kisanuki, Y.Y., et al., *Tie2-Cre transgenic mice: a new model for endothelial cell-lineage analysis in vivo.* Dev Biol, 2001. **230**(2): p. 230-42.

182. Constien, R., et al., *Characterization of a novel EGFP reporter mouse to monitor Cre recombination as demonstrated by a Tie2 Cre mouse line.* Genesis, 2001. **30**(1): p. 36-44.

183. Sato, T.N., et al., *Distinct roles of the receptor tyrosine kinases Tie-1 and Tie-2 in blood vessel formation.* Nature, 1995. **376**(6535): p. 70-4.

184. Sato, T.N., et al., *Tie-1 and tie-2 define another class of putative receptor tyrosine kinase genes expressed in early embryonic vascular system.* Proc Natl Acad Sci U S A, 1993. **90**(20): p. 9355-8.

185. Choi, K., et al., *A common precursor for hematopoietic and endothelial cells.* Development, 1998. **125**(4): p. 725-32.

186. Forde, A., et al., *Temporal Cre-mediated recombination exclusively in endothelial cells using Tie2 regulatory elements.* Genesis, 2002. **33**(4): p. 191-7.

187. Risau, W. and I. Flamme, *Vasculogenesis.* Annu Rev Cell Dev Biol, 1995. **11**: p. 73-91.

188. Minshall, R.D. and A.B. Malik, *Transport across the endothelium: regulation of endothelial permeability.* Handb Exp Pharmacol, 2006(176 Pt 1): p. 107-44.

189. Gavard, J. and J.S. Gutkind, *PRK and ROCK are required for thrombin-induced endothelial cell permeability downstream from galpha 12/13 and galpha 11/q.* J Biol Chem, 2008.

190. Aderem, A. and R.J. Ulevitch, *Toll-like receptors in the induction of the innate immune response.* Nature, 2000. **406**(6797): p. 782-7.

191. Yamaki, K., et al., *Characteristics of histamine-induced leukocyte rolling in the undisturbed microcirculation of the rat mesentery.* Br J Pharmacol, 1998. **123**(3): p. 390-9.

192. Hattori, R., et al., *Stimulated secretion of endothelial von Willebrand factor is accompanied by rapid redistribution to the cell surface of the intracellular granule membrane protein GMP-140.* J Biol Chem, 1989. **264**(14): p. 7768-71.

193. Kubes, P. and S. Kanwar, *Histamine induces leukocyte rolling in post-capillary venules. A P-selectin-mediated event.* J Immunol, 1994. **152**(7): p. 3570-7.

194. Danko, G., et al., *Effect of the PAF antagonists, CV-3988 and L-652,731 on the pulmonary and hematological responses to guinea pig anaphylaxis.* Pharmacol Res Commun, 1988. **20**(9): p. 785-98.

195. Gomez, F.P., et al., *Gas exchange response to a PAF receptor antagonist, SR 27417A, in acute asthma: a pilot study.* Eur Respir J, 1999. **14**(3): p. 622-6.

10 ACKNOWLEDGEMENTS

I would like to express my gratitude to Prof. Stefan Offermanns for giving me the opportunity to do my PhD in his lab in Heidelberg, for his patience, support, and scientific discussions that helped me during my work here.

I would like to thank Alexandra Moers, my supervisor, for introducing me to the world of science, and for always being there for discussions, questions, problems, whether professional or private.

I thank Melanie Bernhard for technical assistance and for improving my German.

All my colleagues I thank for their helpfulness, for nice discussions, for solving my problems together with me, and for friendship.

I am thankful to my parents, Kaija and Jouko, to my sisters, Katriina and Anniina, and to my brother, Aleksi, for their never ending support.

Andreas, without you this all would have been much more difficult.

11 PUBLICATIONS

Submitted publication:

Korhonen, H., Fisslthaler, B., Moers, A., Wirth, A., Habermehl, D., Schütz, G., Wettschureck, N., Fleming, I., and Offermanns, S. (2008). Anaphylactic shock depends on endothelial G_q/G_{11}. Submitted September 2008.

Abstracts:

Korhonen, H., Moers, A.,Wettschureck, N., and Offermanns, S. (2007). The roles of $G\alpha_{q/11}$ and $G\alpha_{12/13}$ in the regulation of the endothelial barrier function. *Naunyn Schmiedberg's Arch. Pharmacol.* 375, Suppl. 1: 34. Abstract.

Korhonen, H., Moers, A., Wirth, A., Wettschureck, N., and Offermanns, S. (2008). The roles of $G\alpha_{q/11}$ and $G\alpha_{12/13}$ in the regulation of the endothelial barrier function. *Basic & Clinical Pharmacology & Toxicology*, Volume 102, Issue s1: 29. Abstract.